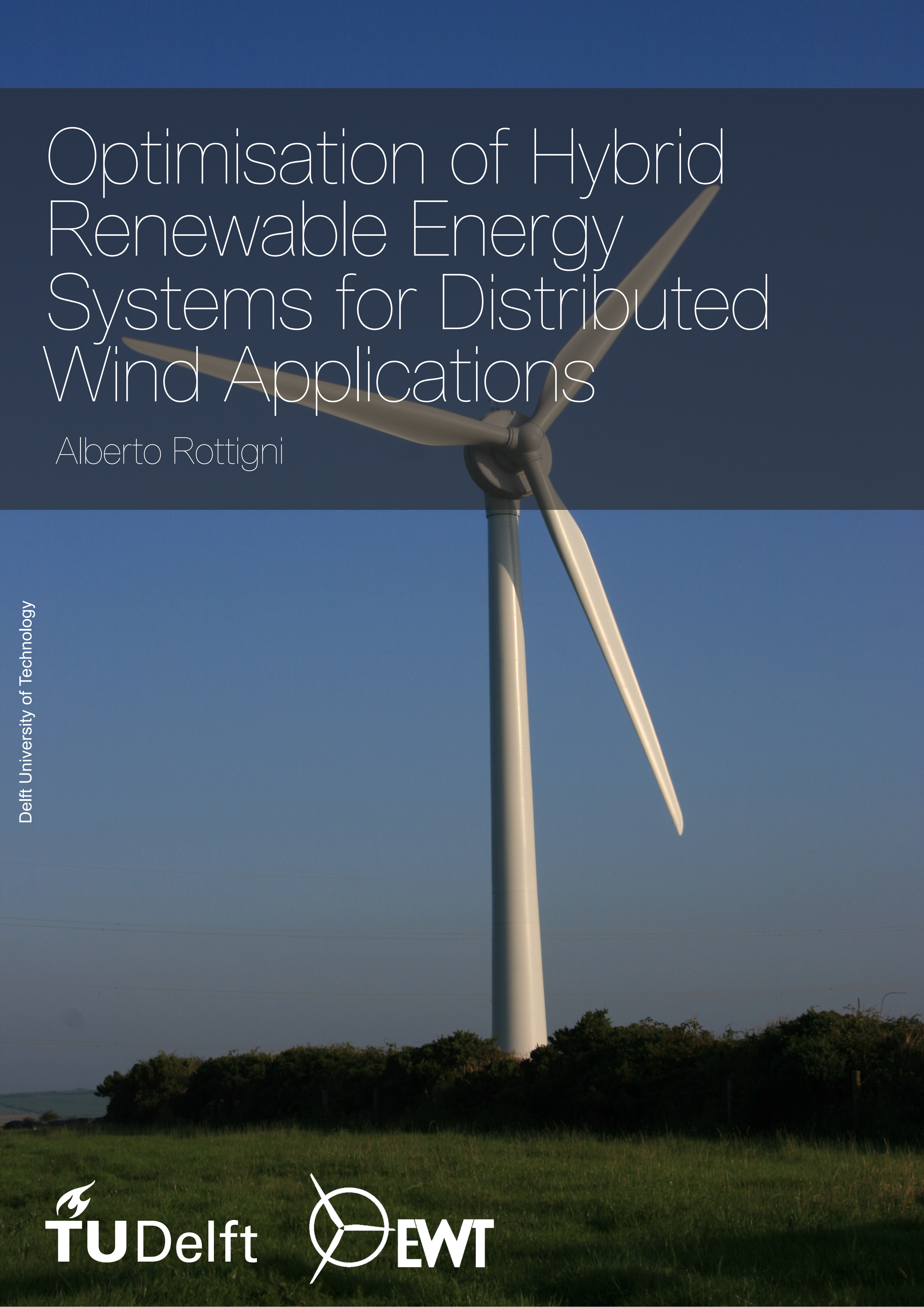

Optimisation of Hybrid Renewable Energy Systems for Distributed Wind Applications

Alberto Rottigni

Delft University of Technology

Optimisation of Hybrid Renewable Energy Systems for Distributed Wind Applications

by

Alberto Rottigni

to obtain the degree of Master of Science
at the Delft University of Technology,
to be defended publicly on 6th of July 2022

Student number:	5351499	
Project duration:	November 19th, 2021 – July 6th, 2022	
Thesis committee:	Prof.dr. D.A. (Dominic) von Terzi	TU Delft, supervisor
	Mr. Mihir Mehta	TU Delft, daily supervisor
	Dr.ir. Laura Ramirez Elizondo	TU Delft
	Mr. Manoj Pathak	EWT
	Mr. Martin Savaris	EWT

Cover: EWT's wind turbine DW-54 500 kW - source: EWT

An electronic version of this thesis is available at `http://repository.tudelft.nl/`.

Acknowledgments

Il primo e più grande grazie va alla mia famiglia, per i tanti sacrifici, il constante supporto e incoraggiamento a rincorrere i miei sogni durante questi 5 anni di studio. Mamma, papà e zio, la mia laurea è la vostra laurea.

Very big thanks to all the people I've shared these two years with. The time spent in Simonsstraat has been an incredible enriching experience and forge of endless memories. I hope there will still be many moments to share and I wish you all guys the life you dream about.

I want to thank Mark Jonkhof, Manoj Pathak, and Martin Savaris. I am extremely grateful for the opportunity you gave me at EWT; I have really appreciated the support you provided and I hope you are satisfied of the work I've done. I would like to thank also my supervisors Dominic Von Terzi and Mihir Mehta, for the inspirational and punctual support.

Last but not the leasts, big thanks to my friends in Italy. Andre, Giù, Ale, Ste and Persi, although 1000 and more kms of distance, I've always felt you close to me. Cheers to us and to many other moments coming.

Alberto Rottigni
Delft, June 2022

Summary

The MSc Thesis Project subject of this report focuses on Hybrid Renewable Energy Systems (HRES), defined as systems made of different energy generation technologies, with at least one of them renewable. HRES' popularity is growing, seen the reduction of both GreenHouse Gases (GHG) emissions and Levelised Cost of Electricity (LCOE) these systems deliver when installed in the right contexts. The project is centered on the application of HRES in the field of distributed wind energy; the choice has been guided by the collaboration with Emergya Wind Technologies B.V., company which designs and manufactures wind turbines with a maximum nominal capacity of 1 MW.

How to optimally design a HRES is still a topic of research. The most diffused commercial software [1] in this field, called Hybrid Optimization Model for Electric Renewables Pro (HOMER Pro), presents some restraints that limit its range of use. With the aim of enlarging the possibilities of the mentioned tool, an optimisation framework to optimally size HRES given inputs, constraints and an objective is written in MATLAB. The code simulates the functioning of an HRES during one year of activity, while exposed to certain weather conditions and serving a given electrical load, to later determine the yearly revenues and project them in the future for the expected project lifetime. A Sequential Quadratic Programming (SQP) algorithm is applied to determine the combination of decision variables which lead to the maximum objective function's value. Three objective functions are carefully studied, precisely:

- Net Present Value (NPV) maximisation;
- Net Present Value (NPV) maximisation when accounting for negative GHG-related externalities;
- System independence maximisation;

Simulations are run on two chosen use cases, with the aim of establishing some recurring trends in the optimisation results. In detail:

1. A grid-connected HRES located in Iglesias (Italy) and operating under the incentive structure regulating so-called ”Comunità Energetiche Rinnovabili” (”Renewable Energy Communities”).
2. An autonomous HRES located in Chumikan (Russian Federation) and relying on a Diesel generator.

The optimisation outcomes show how the optimal HRES size widely vary depending on inputs, costs & revenues structure, and optimisation objectives. When the optimisation aims to maximise the economic performance of the system, the first use case sees an only-solar system as the optimal one. The reason is to associate to a poor wind resource, and consequent high LCOE, for which wind energy is discarded. In the second case study, the integration of wind and solar instead guarantees the most efficient load matching and, consequently, the biggest profit. In both the analysed cases, batteries never result part of the most profitable system when considering the current state of their market. Sensitivity analysis are carried out to understand how external influences can make this technology more economically appealing for this application. Accounting for negative GHG-related externalities suggests how

a carbon tax would impact more the direct emissions of fossil generators, rather than the ones involved in the renewable devices' lifetime. For this reason, the introduction of a taxation system on carbon emissions fosters the installation of renewable energy devices. However, the relaxation of possible constraints on the HRES's maximum nominal capacity is necessary to guarantee the improvement of its economic performance. Finally, when the sizing aims to maximise the system independence, a full hybrid system (wind+solar+batteries) is always the best solution. However, for large electrical loads, the full substitution of fossil based devices becomes problematic.

Contents

Acknowledgments **i**

Summary **ii**

Nomenclature **vi**

1 Introduction **1**

2 Methodology **3**
2.1 Problem Formulation . . . 3
2.2 Objectives . . . 4
2.2.1 NPV Maximisation . . . 4
2.2.2 NPV Maximisation with Negative Externalities . . . 5
2.2.3 System Independence Maximisation . . . 8
2.3 System Modeling . . . 8
2.3.1 Wind Power Production . . . 9
2.3.2 PV Power Production . . . 9
2.3.3 Energy Storage in Batteries . . . 11
2.3.4 Inverter & Rectifier . . . 12

3 Use Case 1: Renewable Energy Communities **14**
3.1 Use Case Description . . . 14
3.2 Optimisation . . . 15
3.3 Environmental Data . . . 19
3.3.1 Wind Resource . . . 19
3.3.2 Solar Resource & Air Temperature . . . 19
3.4 Costs . . . 20
3.4.1 Wind Power Costs . . . 21
3.4.2 PV Power Costs . . . 21
3.4.3 Energy Storage Costs . . . 21
3.5 Results & Sensitivity Analysis - NPV Maximisation . . . 21
3.6 Results & Sensitivity Analysis - NPV Maximisation with Negative Externalities - 27
3.7 Results & Sensitivity Analysis - System Independence Maximisation . . . 31

4 Use Case 2: Autonomous Systems **34**
4.1 Use Case Description . . . 34
4.2 Optimisation . . . 36
4.3 Environmental Data . . . 38
4.3.1 Wind Resource . . . 38
4.3.2 Solar Resource & Air temperature . . . 38
4.4 Costs . . . 40
4.4.1 Wind Power Costs . . . 40
4.4.2 PV Power Costs . . . 40
4.4.3 Energy Storage Costs . . . 41
4.4.4 Generator & Diesel Costs . . . 41

4.5 Results & Sensitivity Analysis - NPV Maximisation 41
4.6 Results & Sensitivity Analysis - NPV Maximisation with Negative Externalities . 44
4.7 Results & Sensitivity Analysis - System Independence Maximisation 46

5 Validation 48
5.1 Validation - Renewable Energy Communities 48
5.2 Validation - Autonomous Systems 49

6 Conclusions 51
6.1 Conclusions - Renewable Energy Communities 51
6.2 Conclusions - Autonomous Systems 52

A Appendix A 55
A.1 Sandia Module Temperature Model 55
A.2 PV Module Technical Sheet 56
A.3 Battery Technical Sheet 56
A.4 Wind Turbine Mass Composition 59
A.5 Provenience of Wind Turbine's Materials 66
A.6 Graphic User Interface 67

B Appendix B - Validation with Homer Pro 72
B.1 Electrical Load - Renewable Energy Communities 72
B.2 PV Modules Power Production - Renewable Energy Communities 73
B.3 Wind Turbine Power Production - Renewable Energy Communities 73
B.4 Exchange with the Grid - Renewable Energy Communities 74
B.5 Costs Summary - Renewable Energy Communities 74
B.6 Electrical Load - Autonomous Systems 75
B.7 PV Modules Power Production - Autonomous Systems 75
B.8 Wind Turbine Power Production - Autonomous Systems 76

Nomenclature

Abbreviations

Abbreviation	Definition
DEP	Diesel Electricity Percentage
EoL	End of Life
EU ETS	European Union Emissions Trading Scheme
EWT	Emergya Wind Technologies B.V.
GUI	Graphic User Interface
HH	Hub Height
HRES	Hybrid Renewable Energy Systems
kWp	kilo Watt peak
LCOE	Levelised Cost of Electricity
MPP	Maximum Power Point
MPPT	Maximum Power Point Tracker
NPC	Net Present Cost
NPV	Net Present Value
PEP	Purchased Electricity Percentage
PV	Photovoltaic
QP	Quadratic Programming
SOC	State of Charge
SQP	Sequential Quadratic Programming
STC	Standard Test Conditions
t	Tonne

List of Figures

2.1 Relative distribution of mass and GHG emissions among each major component of a DW61-900 kW source: EWT . . . 6
2.2 Relative distribution of GHG emissions among each major component of a 1 MWp PV system source: [2] . . . 7
2.3 Schematical representation of the logical steps at the base of the optimisation algorithm . . . 9
2.4 Normalised theoretical wind power curve of a DW61-1 MW . . . 9
2.5 Functioning of the batteries . . . 12
2.6 Schematical representation of a possible system topology Source: Homer Pro 13

3.1 Position of Iglesias, Italy . . . 14
3.2 Load profile types - Case study of Iglesias, Italy . . . 16
3.3 Schematic representation of one iteration of the optimisation process - Case study of Iglesias, Italy . . . 17
3.4 Schematic representation of the revenues computation - Case study of Iglesias, Italy . . . 18
3.5 Working temperature profile of PV modules in one year of functioning - Case study of Iglesias, Italy . . . 20
3.6 Power output of a Hanwha Q.PLUS BFR-G4.1 during one year of functioning and irradiance hitting the optimally tilted module Case study of Iglesias, Italy . 20
3.7 Effect of the average load value change on NPV,IRR & PEP Objective: NPV maximisation - Case study of Iglesias, Italy . . . 22
3.8 Effect of the average wind speed value change on the system size and optimal load composition Objective: NPV maximisation - Case study of Iglesias, Italy . 24
3.9 Effect of the average wind speed value change on NPV,IRR & PEP Objective: NPV maximisation - Case study of Iglesias, Italy . . . 25
3.10 Mean wind speed at 50 m of height in Italy . . . 26
3.11 Carbon permits average price in the EU ETS Source: tradingeconomics.com . 27
3.12 Effect of the carbon tax and average electrical load value on the relative NPV of the optimised system Objective: NPV maximisation - Case study of Iglesias, Italy . . . 28
3.13 Minimum average load to have a DW61-1 MW wind turbine in the optimised system and average load that maximises the economic performance for different average wind velocities. The data is displayed for both the cases when accounting for and neglecting GHG-related negative externalities - Case study of Iglesias, Italy . . . 30
3.14 Effect of the carbon tax and average electrical load value on the relative NPV of the optimised system given a mean wind speed of 5.8 m/s Objective: NPV maximisation - Case study of Iglesias, Italy . . . 31
3.15 Effect of the average load value change on the system size and PEP Objective: PEP minimisation - Case study of Iglesias, Italy . . . 32

3.16 Effect of the average wind speed value change on the batteries' optimum capacity and load division Objective: PEP Minimisation - Case study of Iglesias, Italy . . . 33
3.17 Effect of the average wind speed value change on NPV,IRR & PEP Objective: PEP Minimisation - Case study of Iglesias, Italy . . . 33

4.1 Position of Chumikan, Russian Federation . . . 35
4.2 Electrical load and minimum generator power output - Case study of Chumikan, Russian Federation . . . 35
4.3 Schematic representation of one iteration of the optimisation process - Case study of Chumikan, Russian Federation . . . 37
4.4 Working temperature profile of PV modules in one year of functioning - Case study of Chumikan, Russian Federation . . . 39
4.5 Power output of a Hanwha Q.PLUS BFR-G4.1 during one year of functioning and irradiance hitting the optimally tilted module - Case study of Chumikan, Russian Federation . . . 39
4.6 Relative comparison between the wind turbine related costs in the two analysed use cases . . . 40
4.7 Overall CAPEX for utility-scale PV systems Source: IRENA renewable cost database . . . 41
4.8 Effect of the average wind speed value change on the system size Objective: NPV maximisation - Case study of Chumikan, Russian Federation . . . 42
4.9 Effect of the average wind speed value change on NPV, IRR & DEP Objective: NPV maximisation - Case study of Chumikan, Russian Federation . . . 43
4.10 Effect of the batteries cost change on the system design and DEP Objective: NPV maximisation - Case study of Chumikan, Russian Federation . . . 43
4.11 Effect of the Diesel cost change on the system design and DEP Objective: NPV maximisation - Case study of Chumikan, Russian Federation . . . 44
4.12 Effect of the carbon tax change on the system design and NPV Objective: NPV maximisation - Case study of Chumikan, Russian Federation . . . 46
4.13 Effect of the average wind speed value change on the system size and DEP Objective: DEP minimisation - Case study of Chumikan, Russian Federation . 47

5.1 Comparison between the results obtained with HOMER PRO and the made optimisation framework (referred to as MATLAB) - Case study of Iglesias, Italy 49
5.2 Comparison between the results obtained with HOMER PRO and the made optimisation framework (referred to as MATLAB) - Case study of Chumikan, Russian Federation . . . 50

A.1 Hanwha Q.PLUS BFR-G4.1 Technical Sheet Source: Q Ceels . . . 56
A.2 GUI page 1 . . . 67
A.3 GUI Climate Data . . . 67
A.4 GUI Loads . . . 68
A.5 GUI Technical Economic Inputs . . . 68
A.6 GUI Generator . . . 69
A.7 GUI Wind Turbine . . . 69
A.8 GUI PV Panel . . . 70
A.9 GUI Battery . . . 70
A.10 GUI Converter . . . 71

B.1 Electrical load yearly pattern 72
B.2 Performance of PV Modules 73
B.3 Performance of wind turbines 73
B.4 Exchange with the grid 74
B.5 Actualised costs summary 74
B.6 Electrical load yearly pattern 75
B.7 Performance of PV Modules 75
B.8 Performance of wind turbines 76

List of Tables

2.1 Summary of the carbon footprint of the three main devices of the tested HRES 8

3.1 Values chosen to model the incentive structure - Case study of Iglesias, Italy Source: EWT 15
3.2 Minimum average load to have a DW61-1 MW wind turbine in the optimised system, with related LCOE of wind energy, and average load that maximises the economic performance, for different average wind velocities - Case study of Iglesias, Italy 23
3.3 Optimised system's main features u = 5.8 m/s - Average electrical load = 750 kW 26

4.1 Optimised System's main features - Case study of Chumikan, Russian Federation 42
4.2 Optimised System's Main Features - Case study of Chumikan, Russian Federation 46
4.3 Optimised System's Main Features - Case study of Chumikan, Russian Federation 47

A.1 Temperature coefficients a and b for different module types and mounting configurations Source: [3] 55
A.2 Provenience of the main components of a DW61-900 kW 66

1 Introduction

A fast transition towards sustainable forms of producing, distributing and utilising energy is necessary to stop the rise in temperature and the consequent climate change caused by high concentration of GreenHouse Gases (GHG) in the planet's atmosphere. A Hybrid Renewable Energy System (HRES) is made of different energy generation technologies, with at least one of them renewable. Distributed wind energy is made through wind farms whose overall nominal capacity is limited (20 MW is sometimes recognised as the numeric limit between a distributed and a utility-scale power plant [4]) and which are indeed distributed on the territory. These power plants can be either connected on the customer side of the meter to meet the load or to distribution grids or micro-grids to support grid operations as well as offset large loads located in proximity. This concept opposes the traditional idea of centralised energy production, where the electricity is produced in power plants having a higher nominal capacity, and connected to the distribution grid. The work described in this report focuses on distributed wind-based hybrid energy systems due to the collaboration with Emergya Wind Technologies B.V. (EWT). The mentioned company designs and manufactures direct-drive wind turbines for distributed wind applications; its devices have a maximum nominal capacity of 1 MW. Combining wind, solar, other renewables, and storage in HRES is not only a way of matching electrical loads while reducing the overall GHG emissions but is, in some contexts, the way to deploy electricity at the lowest levelised cost [5]. This point explains the growing commercial interest in these types of energy systems. Moreover, HRES can potentially take diverse advantages to local communities, of which financial savings are the most tangible.

However, how to optimally design a HRES is still a topic of research. The most diffused commercial software ([1]) in this field, called Hybrid Optimization Model for Electric Renewables Pro (HOMER Pro), presents some restraints that limit its range of use. First of all, the optimisation it carries out has the only objective of minimising the Net Present Cost (NPC); other interesting aims, such as Net Present Value (NPV) and system independence maximisation, cannot be treated as objectives of the optimisation. Furthermore, the software does not associate renewable technologies with GHG emissions and, consequently, does not let the user to account for the related negative externalities; for this reason, this tool is not the best when the interest lies in the field of ”True Cost Accounting”.

This work thus aims to answer to the following main research question: *How to optimally size HRES for a given set of inputs, constraints and an objective function?* An answer will be given by developing an optimisation framework, written in MATLAB, that should also overcome some of the limitations of HOMER Pro. To successfully complete the task, a set of research sub-questions is identified:

- What design objectives are interesting from the economic, technical or environmental standpoint?
- What use cases could reflect EWT's commercial interests while giving the opportunity of improving Homer Pro's limitations?
- What are some recurring trends in the obtained optimisation results?

The following lines present the structure of the report. Chapter 2 illustrates the methodology followed in the creation of the optimisation framework, from the problem formulation, to the definition of the optimisation objectives, until the rationale at the base of the code. In particular, this chapter focuses on the aspects of code common to the two treated use cases. Chapter 3 illustrates some features peculiar to the first chosen use case, located in Iglesias - Italy. The optimisation objectives as well as inputs and obtained results are deeply treated in this part. Chapter 4 does the same, but for the second chosen use case, located in Chumikan - Russia. Chapter 5 illustrates how the made optimisation framework has been validated, comparing its outcomes with those of the commercial software HOMER Pro. Chapter 6 concludes the study by drawing a resume of the obtained results, with the objective of underlying some existing trends and make the needed recommendations.

2
Methodology

This chapter describes the methodology applied to meet the objectives of this study. Section 2.1 describes how the problem is formulated from the mathematical standpoint and how the algorithm addresses the optimisation. Section 2.2 illustrates in detail the three investigated objectives of the optimisation. Section 2.3 shows how the system is modelled.

The made optimisation framework is applied to two different use cases. While this chapter focuses on the common aspects of the two, the peculiar features of each use case are treated separately in 3 and 4.

2.1. Problem Formulation

Fmincon is a gradient-based non-linear programming solver able to find the mathematical minimum of a defined function *f(x)*. The optimisation problem is formulated in the following way:

$$min\ f(x)\ s.t. \begin{cases} c(x) \leq 0 \\ c_{eq}(x) = 0 \\ A \cdot x < b \\ A_{eq} \cdot x = b_{eq} \\ lb \leq x \leq ub \end{cases} \tag{2.1}$$

where:

- *x* is a vector.
- *f(x)* is a function that returns a scalar. It can be both linear and non-linear.
- A and A_{eq} are matrices, used to formalise, respectively, a linear inequality constraint and a linear equality constraint.
- b and b_{eq} are vectors, used to formalise, respectively, a linear inequality constraint and a linear equality constraint.
- *c(x)* and $c_{eq}(x)$ are functions that return vectors; they express, respectively, a non-linear inequality and a non-linear equality constraint.
- *lb* and *ub* are vectors, representing the lower and upper bounds to the design vector.

The algorithm uses an iterative process, starting from a user-defined point x_0 and proceeding through following points x_k. The process can be summarised in four steps:

1. **Test for convergence** If the conditions for convergence are satisfied, the optimiser stops and x_k is the optimised solution.
2. **Search direction computation** If the conditions for convergence are not satisfied, the optimiser determines a vector d_k, that defines the direction in the n-dimensions space along which the following point will be searched. n is equal to the length of the design vector.
3. **Step length computation** The optimiser finds a positive scalar a_k, so that $f(x_k + a_k \cdot d_k) < f(x_k)$.
4. **Optimisation variables update** Once found a valid point, the optimiser sets $x_{k+1} = x_k + a_k \cdot d_k$ and $k = k+1$.

Specifically, the algorithm chosen belongs to the Sequential Quadratic Programming (SQP) methods. To solve non-linear programming problems, this class of methods generate, at each iteration, a Quadratic Programming (QP) problem, easily solvable applying any of the QP algorithms. Furthermore, to avoid the display of a local minimum different than the global one, the solver repeats the optimising process starting from various initial points. In the run optimisations, the number of different tested starting points is kept equal to 20. The convergence of 18 of the 20 run optimisations to the same minimum is considered a sufficient condition to declare the found point a global minimum.

Finally, a simple Graphic User Interface (GUI) is created to make the insertion of the needed inputs as user-friendly as possible. Pictures of it can be found in A.6.

2.2. Objectives

The process of sizing HRES is guided by three main optimisation objectives:

- Net Present Value (NPV) maximisation
- Net Present Value (NPV) maximisation with negative externalities
- System independence maximisation

2.2.1. NPV Maximisation

The NPV maximisation is chosen as an objective function seeing the commercial interests of EWT. The NPV is defined as the difference between the present value of cash inflows and that of cash outflows over a time period, and it's used to evaluate a project's profitability: whenever its value is greater than zero, the project is expected to be profitable at the assumed discount rate; the bigger the NPV, the greater the profit expected. On the contrary, if the NPV is lower than zero, the project is foreseen to be unprofitable at the expected discount rate. The NPV is computed through the following formula:

$$NPV = \sum_{n=1}^{N} \frac{R_n}{(1+rd)^n} \tag{2.2}$$

where:

- N is the project lifetime
- R_n is the overall cash flow in year n [€]

- *rd* is the real discount rate [-], calculated as follow:

$$rd = \frac{d - i}{1 + i} \tag{2.3}$$

where:

  - *d* is the interest rate charged to investors for loans [-];
  - *i* is the inflation rate [-];

Another way of evaluating the profitability of an investment is through the Internal Rate of Return (IRR), defined as the discount rate at which NPV equals zero. Whenever the IRR is greater than the expected discount rate, the investment is likely to be profitable; at the contrary, if the IRR is lower than the assumed discount rate, the investment will probably be unprofitable. The IRR is analysed in parallel to the NPV and considered a useful parameter to evaluate the economic performance. However, the two slightly differ in their interpretation. The NPV is indeed more related to the size of the system; for instance, if the HRES size is multiplied by two times, the same holds for the related costs and revenues (or at least for some of them) and, consequently, for the NPV. The maximisation of NPV could thus lead to oversizing systems. On the contrary, the IRR leans towards those projects characterised by a more prudent initial investment. However, the system size in the tested use cases is always kept constrained. For this reason, the NPV, and not the IRR, is chosen to be subject of the optimisation.

2.2.2. NPV Maximisation with Negative Externalities

In an additional extension of the code, negative externalities linked to GHG emissions happening while producing, using and recycling the system's devices are accounted in their economic performance. Extending the possibilities of the code in this direction is considered useful, having noticed how HOMER Pro gives the chance of taxing only direct emissions. Consequently, the negative externalities of all the devices whose functioning does not imply any harmful emission cannot be accounted. The extension of the code subject of this subsection thus aligns the work with the growing interest in the field of "true cost accounting". To do so, the mass of GHG (expressed in tonnes of CO_2 equivalent) emitted during the whole devices' life-cycle is established. As a following step, the amount of emissions of each device is multiplied by a carbon tax value and later accounted in the system's costs. The results of the optimisations carried out for the chosen use cases can be found, respectively, in section 3.6 and 4.6.

In accordance with the information provided by EWT, the overall life-cyle of a DW61-900 kW is linked to the emission of 654.52 t of CO_2eq. The difference between the reference turbine and the DW61-1 MW protagonist of the run simulations regards only the generator and it is considered negligible. Figure 2.1 shows how mass and relative GHG emissions are divided among each turbine's part. The tower and its foundations, being the heaviest of the components (485'432 kg, equal to 88.91% of the total weight), are responsible for around 42% of the emissions. The generator (30'750 kg) follows with 22%. The blades, which are lighter (8'086 kg) but whose production is based on more energy intensive processes, accounts for 17% of total emissions. The mass composition of each wind turbine's component can be consulted in A.

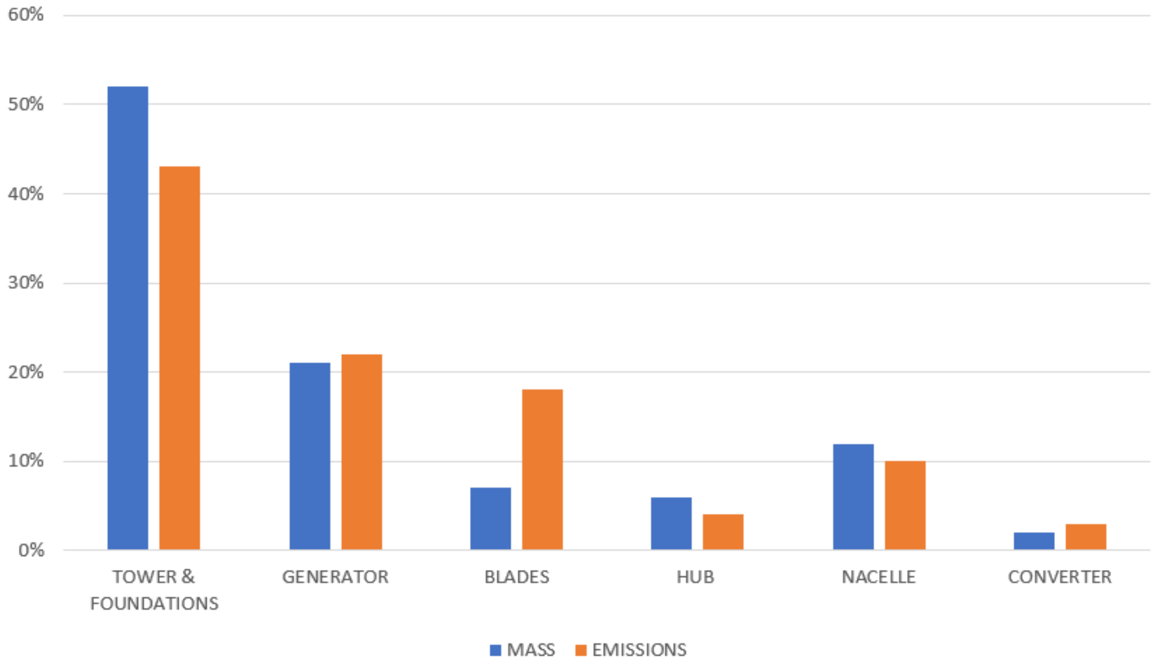

Figure 2.1: Relative distribution of mass and GHG emissions among each major component of a DW61-900 kW source: EWT

An overview of the area of origin of each wind turbine's main component can be found in A.5.

A 1 MWp PV system production, use and End of Life (EoL) generate 563.79 t of CO_2eq. The chosen estimation is retrieved from literature and fruit of a work which studied modules fabricated and used in Germany [2]. Figure 2.2 is a graphical illustrations of the relative distribution of GHG emissions among each component of the system of interest. As can be seen, the cell manufacturing and recycling is responsible for 69% of all the emissions; at the second and third place are the module's frame and glass with, respectively, 12% and 8%.

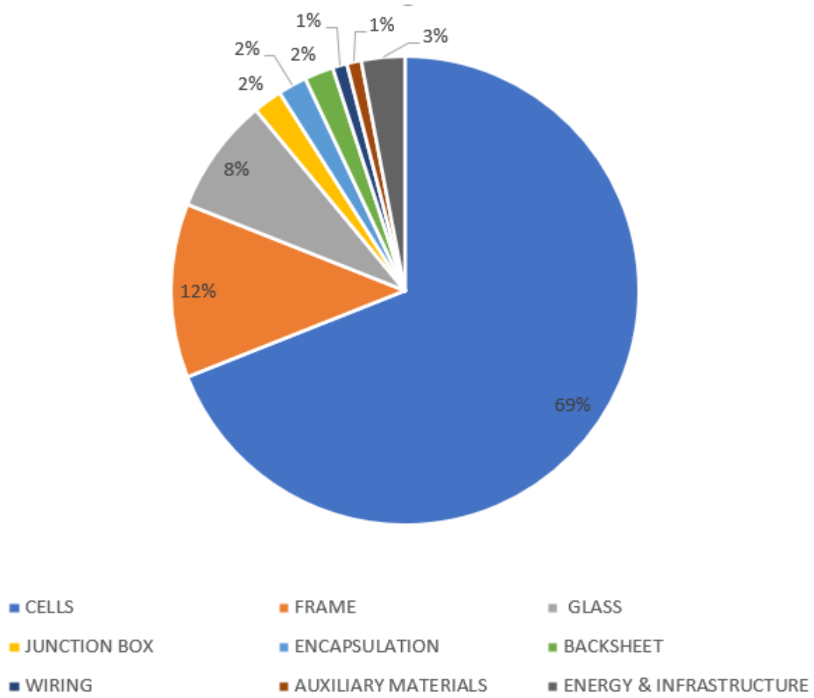

Figure 2.2: Relative distribution of GHG emissions among each major component of a 1 MWp PV system source: [2]

The numbers used to determine the environmental impact of batteries are derived from literature. The European Commission reports a $LiFePO_4$ 79.2 Wh battery to emit 1.2 kg of CO_2eq ([6]). The cells subject to the study are fabricated in Japan, using raw materials coming from China, Taiwan and Thailand; the assembly of the cells and charger, whose overall weight is 0.67 kg, is assumed to happen in Czech Republic; a following travel towards Belgium is considered in order to reach the distribution center. Furthermore, the reported number is influenced by the choice of considering negative externalities related to the electricity flowing into the batteries and its origin. On the contrary, in the made optimisation framework, the electricity, is never bearer of any negative externality, that are associated to only the generation devices. However, seen the complexity of the procedure carried on and its dependence on a large number of assumptions, this aspect is neglected. As a following step, the emissions are deemed proportional to the mass of the device. After estimating the weight of a 1 MWh device equal to 17’727 kg [7], the related GHG emissions are assumed proportional to it. Following this approach, the amount of GHG emitted in the life cycle of a 1 MWh battery results to be 31’749 kg of CO_2eq.

For all the devices, the GHG emissions caused during their lifetime are deemed continuously proportional to their nominal capacity. For instance, a 0.6 MWp PV system is considered to emit 60% of the emissions accounted for the reference 1 MWp system. Life cycle assessments are complex to perform and significantly dependent on the assumptions made. A major role is covered, for example, by the state of the energy systems where the manufacturing of the devices take place, as well as by the consequent international trade. The overall emissions PV modules are responsible for, for instance, would significantly increase if the manufacturing happened in China, where 69.8% of all PV modules were produced in 2020 [8], to later be shipped to Europe. However, the focus when evaluating this extension of the code should be more on the potential of this kind of analysis, rather than on the specific values assumed.

Table 2.1 summarises the amount of CO_2 emitted per each device category.

1 MW Wind Turbine [t CO_2eq/MW]	654.52
1 MWp PV System [t CO_2eq/MWp]	563.79
1 MWh LiFeP0_4 Battery [t CO_2eq/MWh]	31.75

Table 2.1: Summary of the carbon footprint of the three main devices of the tested HRES

When specifically referring to the two implemented use cases, some negative externalities are associated to the electricity purchased from the Italian national grid and the combustion of Diesel fuel. Being these aspects peculiar to the different use cases, further details about the procedure followed can be found in section 3.6 and 4.6.

2.2.3. System Independence Maximisation

For system independence it is meant the capability of the HRES installed to satisfy the load by itself, without relying on other sources of electricity, as for example the national grid or a diesel generator (for more details see 3 and 4). This objective function is chosen because additional to what HOMER Pro can do. The commercial tool indeed offers the opportunity of constraining the capacity shortage and renewable penetration but it does not perform an optimisation guided by their values. While this objective function does not lead to valuable results from the business perspective, it provides interesting insights on how much the system needs to be oversized and on the economic feasibility of it. The optimisation is indeed accompanied by a constraint on the NPV, which can not be lower than zero.

2.3. System Modeling

To determine the optimum solution, the algorithm simulates the system functioning for one year. The length of the unitary time interval the year is divided into is chosen by the user. In the performed simulations, the time interval length is ten minutes; however, the algorithm can work with intervals whose length is comprised between a minimum of one minute and a maximum of one hour. The choice of the step length is often linked to the format of the other available inputs.

Figure 2.3 schematically represents the logical steps at the backbone of the optimisation algorithm. As can be seen, the operations done by the algorithm can be summarised into four conceptual blocks; in the light blue parallelograms the needed inputs, inserted by the user before the optimisation is run, are mentioned. To make this procedure as user-friendly as possible, a simple Graphic User Interface (GUI) is made through MATLAB's app designer; figures showing its structure can be found in A.6. Initially, the solver computes the power production at the time interval of interest; secondly, the algorithm, through a comparison between the electrical demand and production, determines the directions of the electricity flows. As a following step, the revenues for the time step of interest are determined. As anticipated, this sequence (in the orange square in figure 2.3) is repeated for each time interval composing one year. The yearly revenues of the installed HRES are the output of the described operations. Lastly, considering the costs sustained to build and maintain the system as well as the assumed financial parameters, the NPV for the expected project's lifetime can be determined. While the described procedure is the core of the algorithm, the control strategy and revenues calculation differ in the two approached use-cases and are treated separately in 3.2 and 4.2.

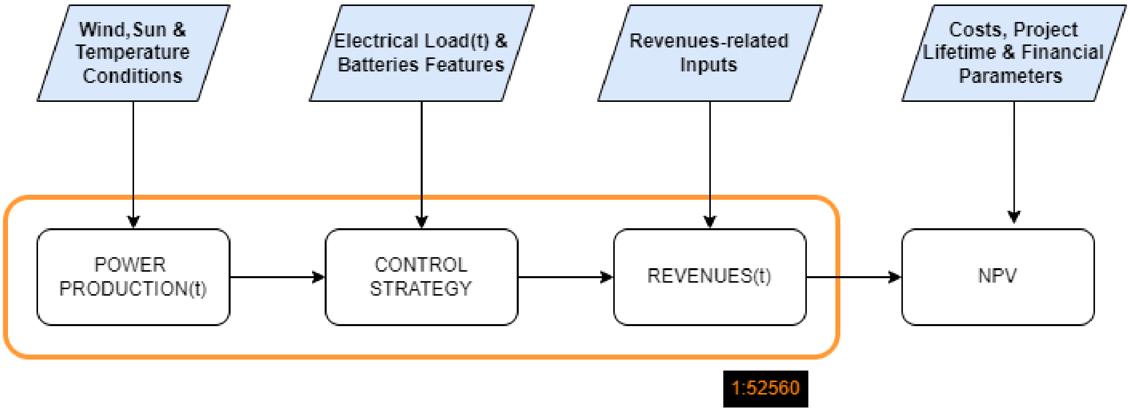

Figure 2.3: Schematical representation of the logical steps at the base of the optimisation algorithm

2.3.1. Wind Power Production

The algorithm computes the wind power production applying the theoretical power curve of a wind turbine. A loss coefficient is heeded to account for losses. In the specific cases, the power curve used is that of an EWT's DW61-1 MW which appears normalised in figure 2.4. With this approach, the wind speed value at each simulated time step is straightforwardly converted into a wind power value.

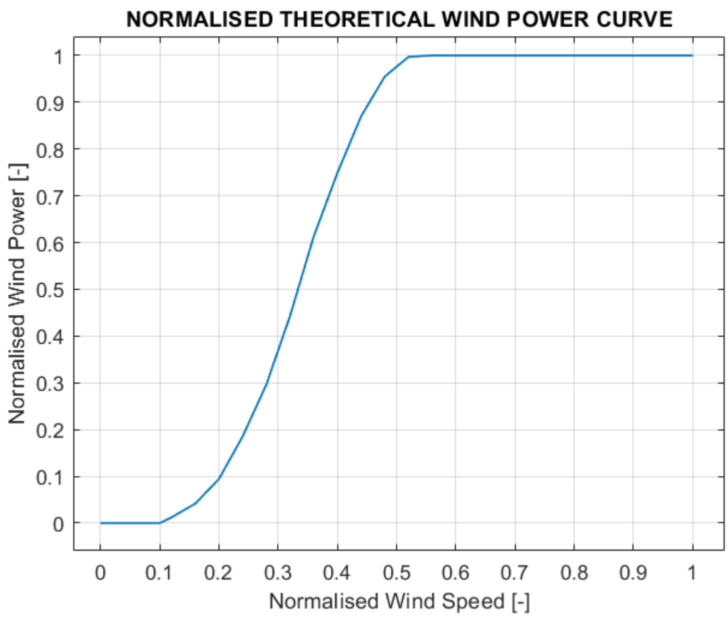

Figure 2.4: Normalised theoretical wind power curve of a DW61-1 MW

2.3.2. PV Power Production

The algorithm computes the PV power production at each simulated time-step, given the solar irradiance hitting the optimally tilted module and considering the module's conversion efficiency, its dependence on the module temperature and some additional losses.

The PV module chosen to run the simulations is a polycrystalline Hanwha Q.PLUS BFR-G4.1, whose nominal power is 280 W. The module is taken from Homer Pro's database, to later be able to validate the production profiles through the software; furthermore, the modest conversion efficiency, equal to 16.80%, is chosen for the costs to accurately represent real ones. Indeed, the higher the conversion efficiency, the higher the module's cost and the further its value from the average. In absence of strict space constraints, opting for the cheaper modules could likely be the most meaningful option. However, an ideal approach would be based on an economic analysis, with the efficiency and number of modules as variables.

The module's temperature is computed applying a model made by *Sandia National Laboratories*, based on two parameters named a and b, which depend on the module construction, materials and mounting configuration. The device has a layer of treated glass as front cover, while one of composite film in the back, underneath the electricity generating cells. The modules are assumed mounted on an open rack. These two features are associated with a temperature coefficient a of -3.56 and a temperature coefficient b of - 0.075 [3]. Different materials and mounting combinations, coupled with the respective temperature coefficients can be found in table A.1. Furthermore, a technical sheet of the chosen module, reporting all the values of interest for the power computation, can be found in A.1.

The following lines illustrate the procedure followed to compute the module temperature and the consequent performance change caused by conditions different than STC. Firstly, the module temperature T_m is computed through the following equation:

$$T_m = G \cdot \exp(a + b \cdot u) + T_{Air} \tag{2.4}$$

where:

- *a* and *b* are the temperature coefficients [-]
- *G* is the overall irradiance hitting the tilted module [W/m^2]
- *u* is the wind speed at 1 metre of height [m/s]
- T_{air} is the air temperature [°C]

After determining the module temperature, the conversion efficiency is computed. Firstly, the open circuit voltage at Maximum Power Point (MPP) $V_{OC-25-G}$, when the module is subject to a temperature of 25°C (thus equal to the one at Standard Test Conditions (STC)) and a certain irradiance, is calculated applying the following equation:

$$V_{OC-25-G} = V_{OC} + \frac{1}{q \cdot n \cdot K_b \cdot T_{STC} \cdot \log(\frac{G}{G_{STC}})} \tag{2.5}$$

where:

- V_{OC} is the open circuit voltage at STC [V]
- *q* is the elementary charge [C]
- *n* is the module's ideality factor [-]
- K_b is the Boltzmann's constant [(m^2· kg)/(s^2· K)]
- T_{STC} is the temperature at STC [K]
- G_{STC} is the overall irradiance hitting the module at STC [W/m^2]

As a following step, the short circuit current of the module $I_{SC-25-G}$ at MPP and same conditions aforementioned, is computed starting from the same physical quantity at STC, I_{SC}, through the following equation:

$$I_{SC-25-G} = I_{SC} \cdot \frac{G}{G_{STC}} \tag{2.6}$$

Consequently, the power produced by the module at Maximum Power Point (MPP), and given the mentioned environmental conditions $P_{MPP-25-G}$, is obtained:

$$P_{MPP-25-G} = V_{OC-25-G} \cdot I_{SC-25-G} \cdot FF \tag{2.7}$$

where *FF* is the fill factor [-], whose value is assumed not to be influenced by the module temperature and irradiation.

The module efficiency at those conditions Eff_{25-G} is retrieved through the following formula:

$$Eff_{25-G} = \frac{P_{MPP-25-G}}{G \cdot A} \tag{2.8}$$

where *A* is the module's active surface. The relation between the efficiency at 25 °C and that at a different temperature *T* when the module is hit by the irradiance *G* is expressed by the equation below:

$$Eff_{T_m-G} = Eff_{25-G} \cdot (1 + k \cdot (T_m - 25)) \tag{2.9}$$

with *k* being the temperature coefficient for the module's efficiency [-/°C]. Finally, the PV power produced by the module when hit by the irradiance *G* at a temperature T_m is calculated:

$$PV_{Power} = Eff_{T_m-G} \cdot 0.96 \cdot G \cdot A/1000; \tag{2.10}$$

where 0.96 accounts for additional losses (MPPT, modules mismatch, cables and soiling).

2.3.3. Energy Storage in Batteries

The batteries are modeled considering the energy capacity, the State Of Charge (SOC) and a power limit on charge and discharge. In case the electricity production is greater than the one demanded, the controller verifies if some of (or all) the excess electricity can be stored in batteries. This is done by checking the SOC, that cannot be higher than the maximum allowed, expressed by the user. In the performed optimisation, this value is assumed to be 100%. In the case some of (or all) the excess electricity can be stored into batteries, an additional constraint on the power flowing into the devices is applied. Indeed, the power flow cannot overcome a set limit, assumed equal to 1 MW in the performed optimisations. Furthermore, a loss of 5% is considered when charging the batteries. In case the electricity production is lower than the demanded one, energy can be taken from the batteries. An initial check on the SOC, that cannot be lower than the minimum allowed, is done by the controller. In the executed simulations, this value is considered equal to 10%. In a similar way to what done in the previous case, a limit on the power flow when discharging the batteries, assumed equal to 1 MW, is applied. The reported values are taken from the battery FREQCON MSC 1000 Wind, whose technical sheet can be consulted in A.3. An additional loss of 5% is heeded when discharging the batteries. At each simulated time-step, the SOC of the batteries is updated accordingly to the amount of energy flowing in or out the storing devices.

Finally, the batteries are modelled without any specific reference to an existing device. In the optimisation, the energy capacity can indeed assume any value between the lower and upper limits specified by the user. No temperature effects are considered, in the belief the batteries would come with a cooling system able to keep the temperature constant in order to optimise the devices' performance. In case this assumption revealed to be not true, some changes should be made for a more accurate description of reality. The flowchart reported in 2.5 illustrates the explained rationale behind the functioning of the batteries.

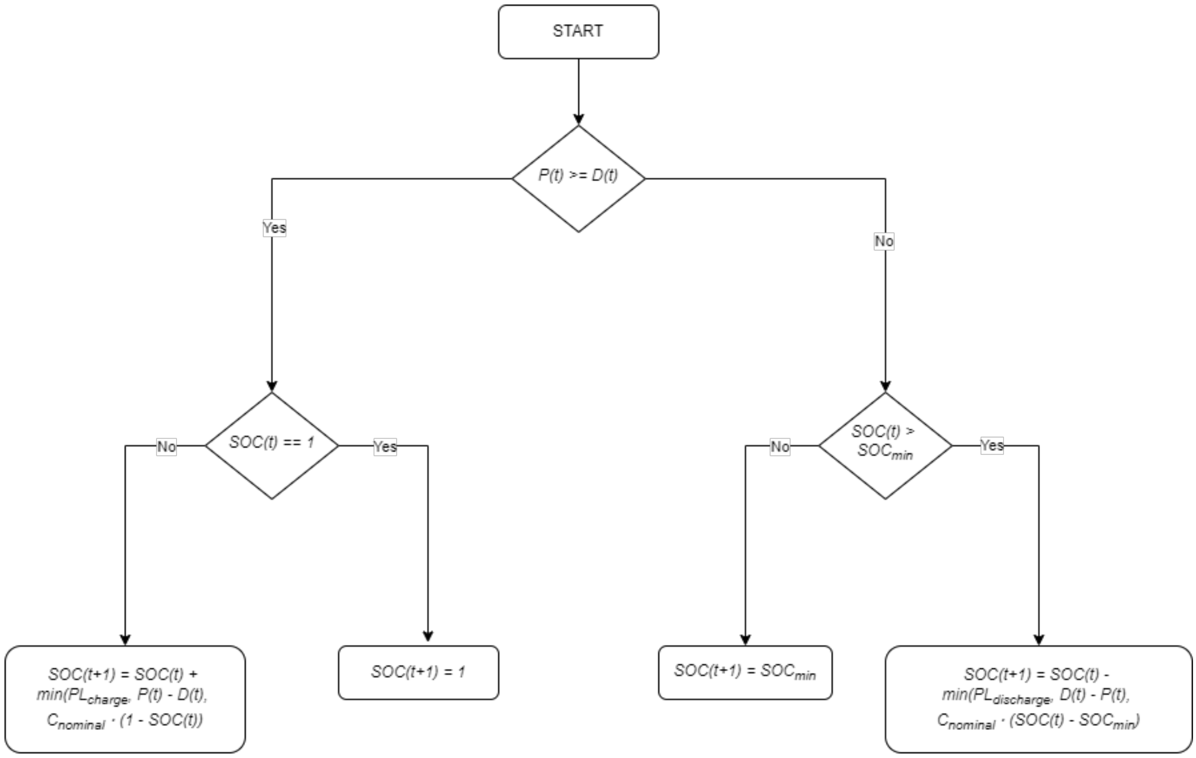

Figure 2.5: Functioning of the batteries

where:

- *P(t)* and *D(t)* are, respectively, the electricity production and demand at the simulated time-step t;
- *SOC* indicates the batteries' State of Charge;
- SOC_{min} is the minimum SOC allowed (assumed in the model to be 0.1);
- PL_{charge} is the maximum power that can flow into the batteries when charging them (PL stands for Power Limit). When updating the batteries' SOC, this power value is converted into an energy value;
- $PL_{discharge}$ is the maximum power that can flow into the batteries when discharging them (PL stands for Power Limit). When updating the batteries' SOC, this power value is converted into an energy value;
- $Capacity_{nominal}$ is the nominal energy capacity of the storing devices;

2.3.4. Inverter & Rectifier

While the wind turbines produces AC current, the PV modules and batteries work with DC. Similarly, the load is assumed to be AC-type. Consequently, an inverter is needed when the current flows from the modules or batteries towards the load. The inverter converts DC current into AC current. At the contrary, a rectifier is necessary while the current flows from the turbines to the batteries. This device converts the current from AC to DC. In the model, both the inverter and rectifier are taken into account trough the computation of the losses occurring when the electricity flows trough them. For both the devices, an efficiency of 98.3% is assumed.

This value is taken from the battery FREQCON MSC 1000 Wind that comes equipped with an inverter; its technical sheet can be consulted in A.3. The devices are considered as always able to handle the power flow, and thus correctly sized. A more detailed model should accurately capture the dynamics of the power flow; however, this is not the scope of the study. Figure 2.6 provides a schematic representation of one of the system topologies; both the converter and rectifier are assumed to be represented by the box named *Converter*.

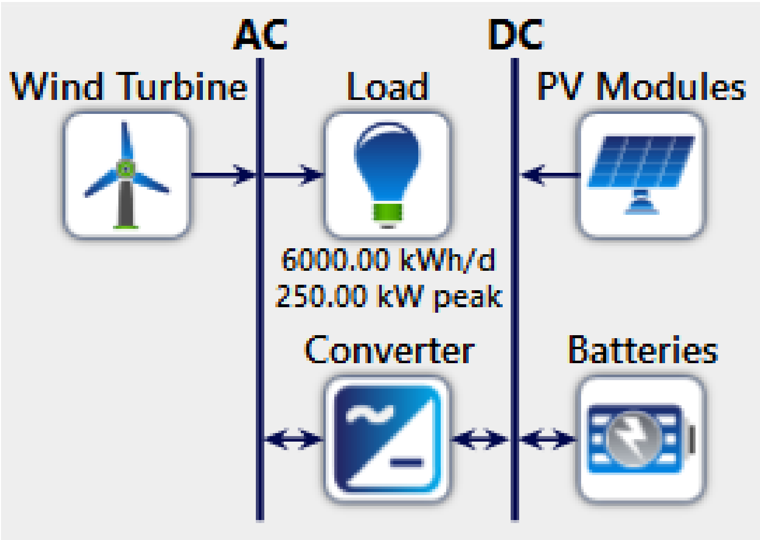

Figure 2.6: Schematical representation of a possible system topology
Source: Homer Pro

3

Use Case 1: Renewable Energy Communities

This chapter provides the necessary insights about the first of the chosen use cases. Section 3.1 gives an overview of it, with the main characteristics and reasons the use case has been chosen for. Section 3.2 describes the optimisation procedure, defining the variables subject to the optimisation as well as depicting the simulation of the system functioning. Section 3.3 displays the environmental data used to compute the devices' power production while section 3.4 illustrates the investments to carry out to implement and maintain the HRES. Finally, section 3.5, 3.6 and 3.7 illustrates the results of the performed optimisation and sensitivity analysis for each optimisation objective.

3.1. Use Case Description

The use case of interest is located in Iglesias, a medium-sized town in the southern part of Sardinia. Figure 3.1 shows its position on the map.

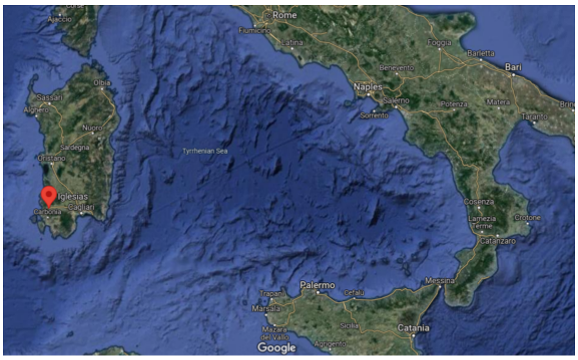

Figure 3.1: Position of Iglesias, Italy

This use case is representative of one of so-called "Comunità Energetiche Rinnovabili" (meaning "Renewable Energy Communities") that would be likely to spread if the incentive system, currently in the pipeline, was officialised. The relative incentive structure would reward consumption of electricity locally produced from renewable energy sources. The purpose of this policy would be that of fostering the growth of renewable energy production while decreasing grid saturation. A growth of distributed generation devices would indeed be accompanied by a drop in the necessary supply from the national grid. Thanks to the mentioned incentive, the members of these communities would have access to an additional cash flow that would cover the investment needed to purchase the HRES and take additional benefits to local communities and their territory. Table 3.1 shows the values chosen to model the incentive structure; the regular electricity price is assumed equal to last 10 years average [source: EWT].

Incentive	0.13 €/kWh
Regular Electricity Price	0.056 €/kWh
Discount on Electricity Price at Night and Weekends	10%

Table 3.1: Values chosen to model the incentive structure - Case study of Iglesias, Italy
Source: EWT

In more detail, the incentive would reward self-consumption referring to the minimum measured at each hour. In the built model, a wind and a solar power plant serve the community; their nominal capacity, according to the regulation of ”Renewable Energy Communities”, is constrained to 1000 kW. This use case is considered of interest seen the impossibility of modeling the rewarding tariff on self-consumption through HOMER Pro. Furthermore, the existence of a constraint on the plants' nominal capacity makes this case aligned with the features of distributed energy plants and thus to EWT's commercial interests.

3.2. Optimisation

The variables subject to optimisation are the following:

- x_1 : nominal wind capacity [kW]
- x_2 : nominal PV capacity [kW]
- x_3 : nominal batteries energy capacity [kWh]
- x_4 : percentage of industrial load-type [%]
- x_5 : percentage of community load-type [%]
- x_6 : percentage of commercial load-type [%]

Each optimisation variable is normalised with respect to the difference between the respective upper and lower limit, for the optimiser to be faster and more precise. For this reason, each variable is bounded between 0 and 1. The first three variables represent the system size. The second three refer to the load pattern. Indeed, especially when the objective is maximising the NPV, self-consumption, and consequently, the revenues coming from the incentive, must be maximised. Adapting the load pattern, given its average value as a required input, to have it resembling the production pattern as much as possible, can increase the returns. To do so, the code combines three already known load profiles, specifically:

- Community load profile: characterised by two typical peaks, with the evening one more pronounced.

- Industrial load profile: always constant, apart from some oscillations.
- Commercial load profile: constant during working hours while lower and flatter at night.

Figure 3.2 shows a representation of each load pattern in a day for an average load value of 250 kW; each load type is characterised by random oscillations, used to account for uncertainties and unpredicted changes.

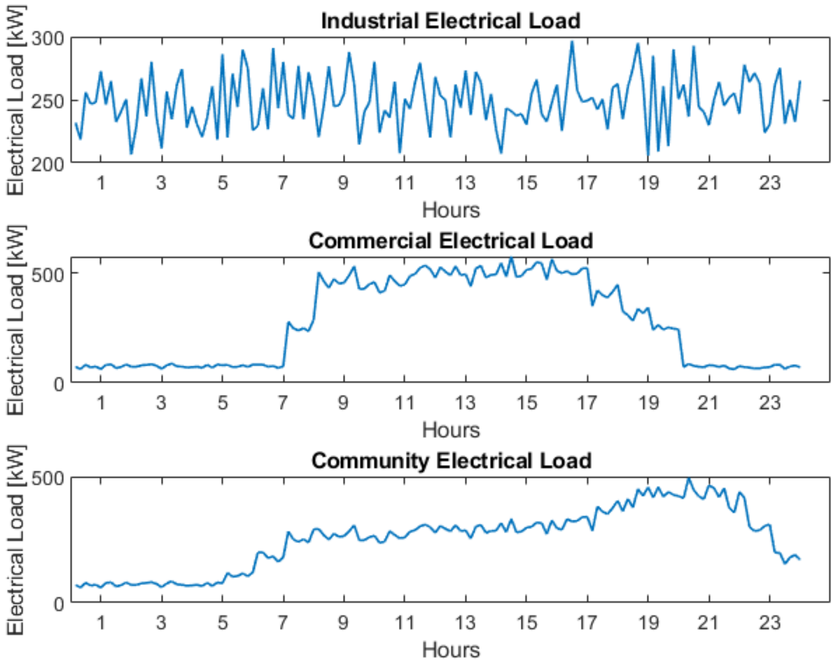

Figure 3.2: Load profile types - Case study of Iglesias, Italy

The optimiser returns the percentage of each load profile which composes the optimal electrical load. This is a useful indication for EWT that, thanks to this information, knows not only how to size the system but also what kind of clients to look for to maximise its profits. Additional value to this approach is given by the limitations of Homer Pro, which can only consider the electrical load as a fixed input.
The flowchart in figure 3.3 schematically illustrates one iteration of the optimisation process. The optimisation variables can be found in the green parallelograms while the blue ones contain fixed required inputs.

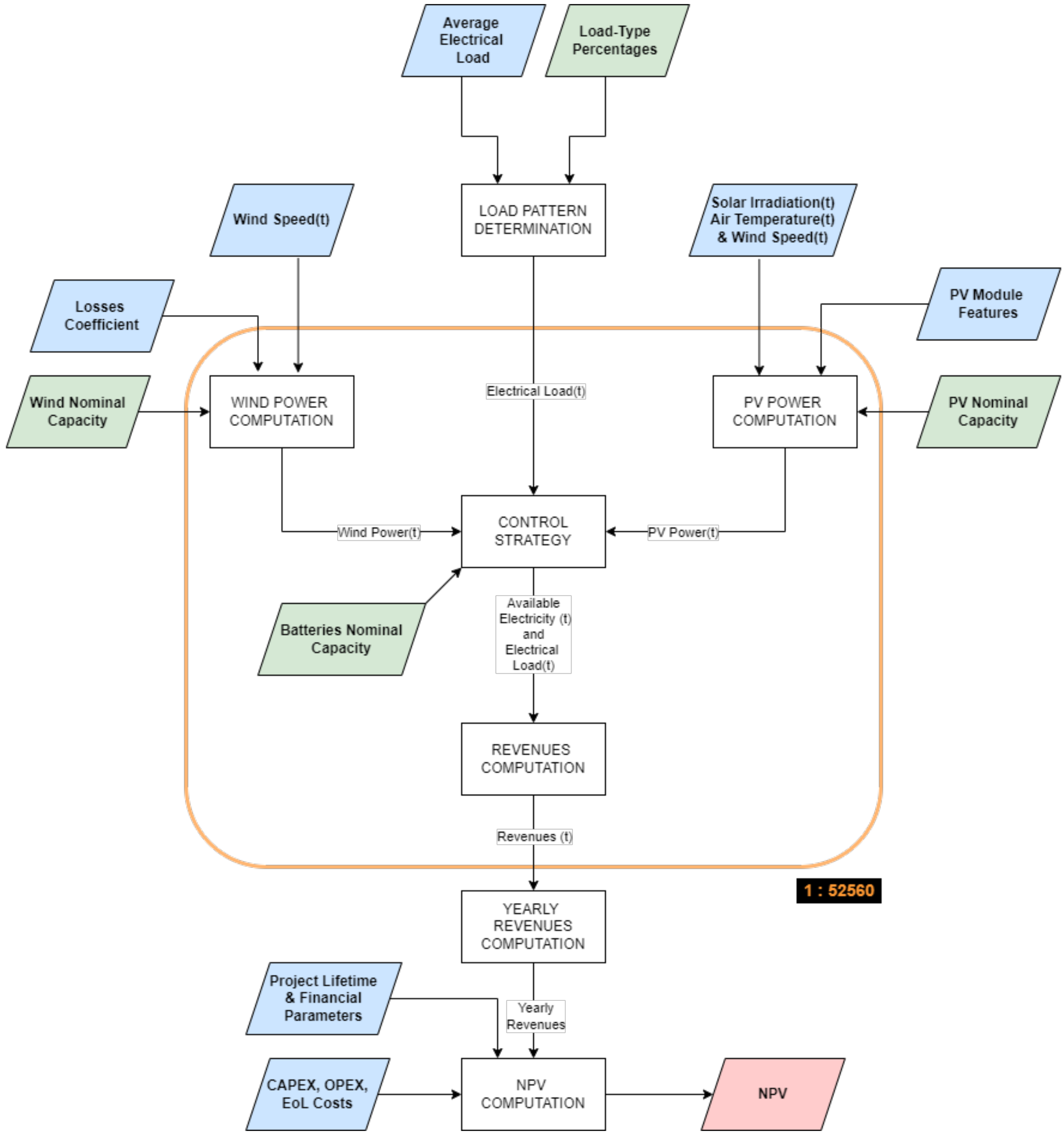

Figure 3.3: Schematic representation of one iteration of the optimisation process - Case study of Iglesias, Italy

Starting from the environmental conditions, the optimiser computes the wind and PV energy production at a certain time step (see 2.3.1 and 2.3.2 for a detailed description of these computations). In the *CONTROL STRATEGY* block, the algorithm establishes the direction of the different electricity flows, starting from the comparison between the electricity produced and the demanded one. Having the objective of maximising the revenues coming from the incentive, the plant's control strategy prioritises the load matching. In case of an overproduction of electricity, the excess amount is sent to batteries; this priority order is chosen to make the system the most resilient to drops of renewable energy production and, consequently, to limit as much as possible the purchase of electricity from the grid. If the energy or power limit is exceeded, the energy which cannot be stored is sold to the grid for the regular electricity price. In case of an underproduction of electricity, the algorithm checks the availability of stored energy in the batteries and, heeding the energy and power constraints (see 2.3.3), determines if the load can be satisfied with it. Once the direction of the electricity flows is established, the optimiser (in the *REVENUES COMPUTATION* block) compares the electricity coming from the power plant (either from wind turbines, PV modules or batteries) with the maximum amount of self-consumed electricity which can be rewarded with the incentive. This comparison is necessary to establish the revenues coming from the incentive given for self-consumption. A following comparison with the electrical load to match is necessary in order to establish if some electricity has to be acquired from or sold to the national grid; consequently, revenues (or costs) other than the incentive are drawn. The rationale behind the calculation of the revenues at each time step is displayed in the flowchart in figure 3.4.

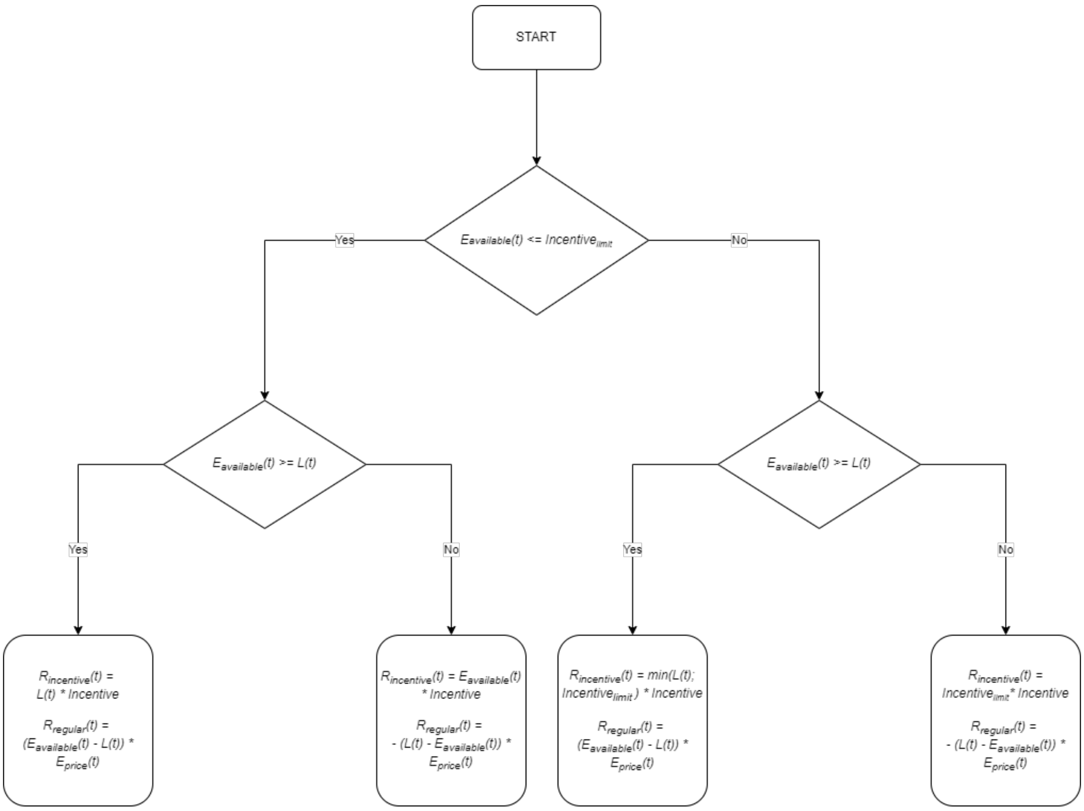

Figure 3.4: Schematic representation of the revenues computation - Case study of Iglesias, Italy

where:

- $E_{available}$*(t)* refers to the electricity coming out of the power plant at time step t.
- *Incentive*$_{limit}$ indicates the maximum amount of self-consumed electricity rewarded with the incentive.
- *L(t)* is the electrical load at time interval t.
- *Incentive* indicates the economic reward per kWh of electricity produced and self-consumed by the community.
- E_{price}*(t)* indicates the price to purchase from or sell electricity to the national grid at time instant t.
- $R_{incentive}$*(t)* is the revenues coming from the incentive in time interval t.
- $R_{regular}$*(t)* relates to the cash flow linked to the purchase or sale of electricity from/to the national grid.

The incentive structure rewards the minimum self-consumption measured at each hour. As an example, if in 50 minutes out of 60, the HRES produces 100 kWh to be consumed by the community while in the last 10 minutes the production of the system is null, no revenues will be given to the community for the hour of interest. To represent this fact, after having computed the revenues at each simulated time step, the solver compares all the incentive revenues at each hour and aligns them to the minimum one.

The blocks in the orange square displayed in the flowchart in figure 3.3 are repeated for each simulated time step (52560 times in the case the chosen interval duration is 10 minutes). The outcome is a scalar representing the revenues in one year of functioning of the system. Given the interest rate charged by investors for loans and the inflation rate, the yearly revenues are actualised for each year falling into the expected project lifetime (equal to 25 years in the performed optimisation). When the same is done with the costs, an actualised cash flow is obtained for each year of the project lifetime. Consequently, the NPV is computed (see 2.2.1 for further details about the performed calculations).

The aforementioned procedure shows how the algorithm determines the NPV for one combination of variables subject to the optimisation. As explained in 2.1, if the conditions for convergence are not respected, the algorithm repeats the process for different values of these variables. The iterations stop whenever the conditions for convergence are respected and the optimal combination of the variables subject to optimisation is found.

3.3. Environmental Data

This section displays the environmental data used to compute the devices' power production.

3.3.1. Wind Resource

According to simulations internally carried out by EWT, the average wind speed at hub height (HH = 84 m) in the location of interest is 5.3 m/s. Not having access to direct measurements for the wind speed at hub height in Iglesias, the wind velocity time series is assumed to be equal to that of another Italian location (precisely, Masseria del Duca). This wind pattern is later adapted to obtain the cited average wind speed. The obtained time series corresponds to a Weibull distribution described by scale and shape parameter of, respectively, 5.9934 and 1.9478. The wind resource in Iglesias thus results to be quite poor, with a hypothetical DW61-1 MW's capacity factor of only 19.67%.

3.3.2. Solar Resource & Air Temperature

The direct, diffused and reflected irradiance hitting the optimally tilted (33°) module and the air temperature data is obtained from [9]. The overall irradiation hitting the device in one year is 1938 kWh/m^2. Figure 3.5 shows the module temperature pattern during one year of work.

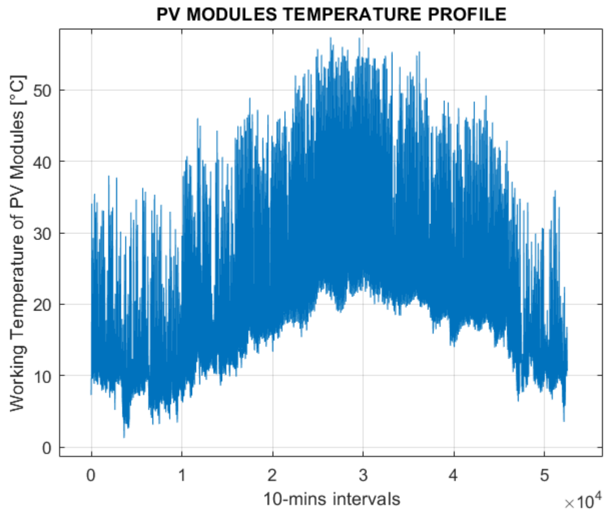

Figure 3.5: Working temperature profile of PV modules in one year of functioning - Case study of Iglesias, Italy

The environmental conditions the PV modules are exposed to in Iglesias make their average working temperature equal to 21.71 °C. The maximum and minimum working temperatures are, respectively, 57.36 °C and 1.24 °C. Accordingly, the modules efficiency oscillates between 14.72% and 18.27%. Figure 3.6 shows the power output profile of one PV module opposed to the irradiance hitting the optimally tilted module and the relation between the two. As expected, the module power output is on average greater during summer months.

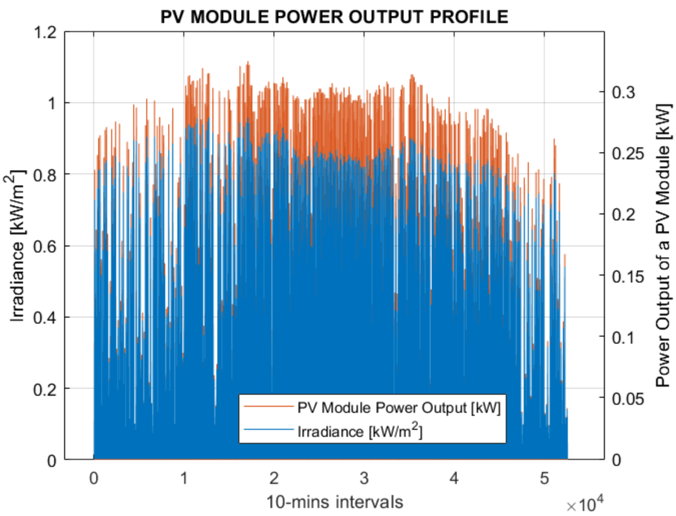

Figure 3.6: Power output of a Hanwha Q.PLUS BFR-G4.1 during one year of functioning and irradiance hitting the optimally tilted module Case study of Iglesias, Italy

The module's capacity factor results to be 20.31%.

3.4. Costs

This subsection reports the CAPEX,OPEX and End of Life (EoL) costs used to account for the investments carried out to make and maintain the system.

3.4.1. Wind Power Costs

CAPEX,OPEX and EoI costs of a DW61-1 MW are provided by EWT and they are subject to non-disclosure agreement.

3.4.2. PV Power Costs

A CAPEX of 1067 \$/kWp (≈ 950 €/kWp) and an OPEX of 10 \$/kWp is considered [10]. 2020's average costs are preferred to 2021's, because thought to be more representative of a future situation, as they ignore the volatility that occurred in 2021 due to supply chain complications and rising commodity prices [11]. The reported costs include the expenses for the converter.

3.4.3. Energy Storage Costs

The batteries' CAPEX is considered to be 550 €/kWh [12] while the OPEX is assumed equal to 10 €/kWh [source:EWT]. The reported costs include the expenses for the converter. Being the project lifetime 25 years, while that of the batteries assumed equal to 15 years, an EoL cost to substitute the batteries at the end of their lifetime and to continue having them as part of the system is needed. Seeing the expected dip in batteries' price in the coming years, using the same CAPEX value would not be representative of a real situation. Instead, a value of 396 €/kWh, representing a reduction of 28% in 15 years (conservative scenario according to [13]) is inserted.

3.5. Results & Sensitivity Analysis - NPV Maximisation

For the described use-case of Iglesias, the HRES that maximises the NPV, regardless of the average load value inserted, is a 1 MW only-solar system. Solar energy results particularly favoured by the abundant availability of irradiation, which makes the LCOE equal to 0.026 €/kWh. Furthermore, the load profile is entirely made by the commercial pattern type. The reason for this is the closest similarity between the production and demand pattern, which maximises the revenues coming from the incentive.

The reason for wind power not to be part of the most profitable system is the wind resource's scarcity that leads to a low capacity factor (19.67%) and thus to a poor electricity production (1.71 GWh/year). As a consequence, the LCOE of wind energy made from a DW61-1 MW is 0.067 €/kWh, around two point five times higher than that of solar energy. As a consequence, the addition of a wind turbine would cause a decrease in NPV. In addition, no batteries are part of the system.

It is interesting to notice how the change in the average load value affects the results; figure 3.7 shows this cause-effect relation. The higher the average load value, the greater the NPV and IRR. While the electricity produced by the installed PV modules stay constant, the amount of it which is self-consumed increases, with a parallel decrease in the quantity sold to the grid for the regular electricity price. The overall effect is a growth in revenues coming from the incentive and, consequently, of the financial parameters. PEP stands for ”Purchased Electricity Percentage” and indicates the load matched by purchasing electricity from the national grid. The latter is calculated through the following equation:

$$PEP = \frac{E_{purchased}}{L_{total}} \tag{3.1}$$

where:

- $E_{purchased}$ indicates the yearly load matched by purchasing electricity from the grid [kWh]

- L_{total} is the annual electrical load [kWh]

The increment of PEP is easily explainable by the rise in the required electricity, while the production stays constant. The maximum average load appearing in the graph (1000 kW) is the one which guarantees all the electricity produced to be self-consumed. Consequently, opting for a greater mean load does not make sense: while the PEP would increase, the economic parameters would stay the same. Finally, whenever the load value overcomes this number, the load profile optimisation loses significance. Indeed, several different load profiles, being that production is often lower than demand, lead to the same economic performance.

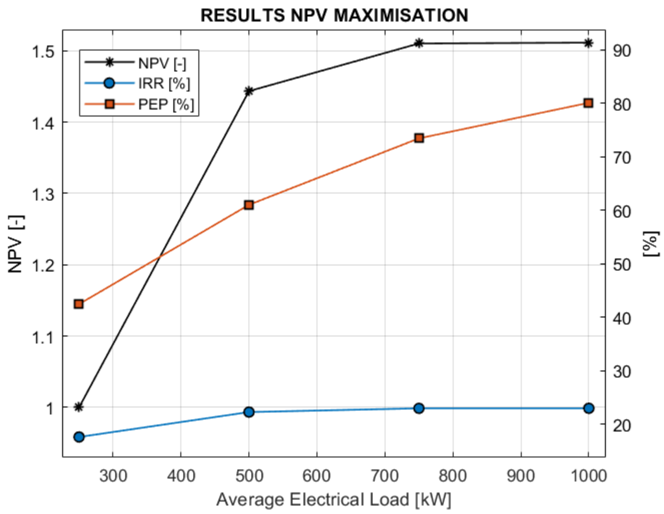

Figure 3.7: Effect of the average load value change on NPV,IRR & PEP
Objective: NPV maximisation - Case study of Iglesias, Italy

Being EWT interested in wind-based systems, a sensitivity analysis on the mean wind speed is carried out with the interest of seeing which of its values caused wind power to get integrated into the optimal system. To do so, the wind velocity pattern is adapted changing the average wind speed from 5.3 to 7.3 m/s. The interval falls into the limits for a class III wind turbine, made to stand a maximum average wind speed of 7.5 m/s. With u the mean wind velocity:

- u $\leq$ 5.55 m/s : the most profitable system is an only-solar one for every average load value.
- u $\geq$ 5.55 m/s : wind power starts to get integrated into the system, with a DW61-1 MW wind turbine part of the optimised system for certain values of the average load.
- u $\geq$ 6.8 m/s: a DW61-1 MW wind turbine is always part of the optimised system.

Table 3.2 shows, for each average wind speed, the minimum average load to have a DW61-1 MW in the most profitable system, with related LCOE of wind energy, and the mean load which maximises the economic performance. The latter results to be the one for which all the electricity produced is self-consumed. For this reason, as already anticipated, a further increase in the average load would not take to any improvements of the economic performance. As can be seen, a DW61-1 MW wind turbine is part of the optimised system whenever the related LCOE is lower than 0.054 €/kWh. The optimisation outcome is here influenced by the constraint on nominal capacity as well as by the incentive structure. The latter indeed introduces a difference in each kWh's value; specifically, a kWh which is self-consumed is worth more than one that is, for instance, sent to the grid. Consequently, it is more meaningful to install a wind turbine rather than additional cheaper solar panels when the additional electricity produced increases the self consumption enough to maximise the overall profit. Furthermore, the constraint on nominal capacity, once reached, prevents the installation of additional PV modules and opting for the most expensive technology becomes a necessity. Finally, an improved wind resource causes an increase in the amount of electricity produced and a further drop in LCOE's value.

Average Wind Speed [m/s]	Minimum Average Load [kW] - LCOE Wind [€/kWh]	Optimal Average Load [kW]
5.3	-	-
5.55	1250 - 0.054	1750
5.8	750 - 0.048	1750
6.05	750 - 0.046	1750
6.3	500 - 0.042	1750
6.55	500 - 0.039	1750
6.8	250 - 0.037	1750
7.05	250 - 0.034	1750
7.3	250 - 0.033	1750

Table 3.2: Minimum average load to have a DW61-1 MW wind turbine in the optimised system, with related LCOE of wind energy, and average load that maximises the economic performance, for different average wind velocities - Case study of Iglesias, Italy

Figure 3.8 shows how the change in the mean wind speed impacts the system size and the optimal load pattern. The cases represented are those for which the average load value is the one which maximises the profits. As can be seen, the optimal wind capacity goes to 1 MW whenever the average wind velocity surpasses 5.55 m/s, while the optimal PV capacity is always equal to its upper limit. The addition of a 1 MW turbine translates into a more equal division of the load pattern between the industrial and commercial load profile. With a commercial load profile, indeed, a good part of electricity coming from the wind turbine could not be consumed at night, limiting the revenues from the incentive. The community load profile never contributes to shape the optimal load pattern. Indeed, the night electricity requirement is too low to consume the wind electricity available. At the same time, its morning profile resembles less the solar power production when compared with the commercial load profile.

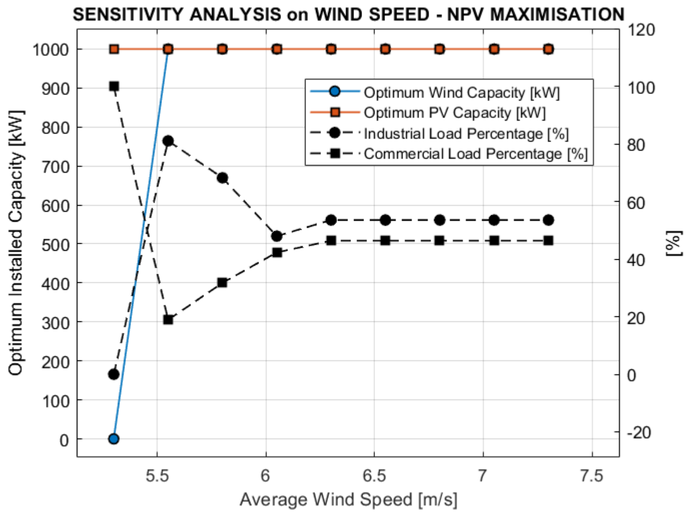

Figure 3.8: Effect of the average wind speed value change on the system size and optimal load composition Objective: NPV maximisation - Case study of Iglesias, Italy

Finally, figure 3.9 shows the impact of a changing average wind speed on the techno-economic parameters used to evaluate the system performance. As expected, for those cases with an optimised average load value, the greater the wind speed, the greater the NPV & IRR, while the lower the PEP. Indeed, a better wind resource causes an increment in the wind turbine's capacity factor and, consequently, a reduction in its LCOE. Furthermore, the higher the wind turbine production, the more demand is matched and the greater the revenues coming from the incentive. The dip in IRR when passing from an average wind speed of 5.3 to 5.55 m/s is linked to the wind turbine addition which takes a higher initial investment; indeed, a greater initial expense makes the profitability of the project more sensitive to a growth of the expected discount rate. For this reason, the IRR results to be lower than that of an only-solar system. Ultimately, batteries are never part of the HRES that maximises the profits; this happens simply because, in the case with the average load value as high as possible to maximise the revenues, all the electricity is already self-consumed and none of it would meaningfully be stored.

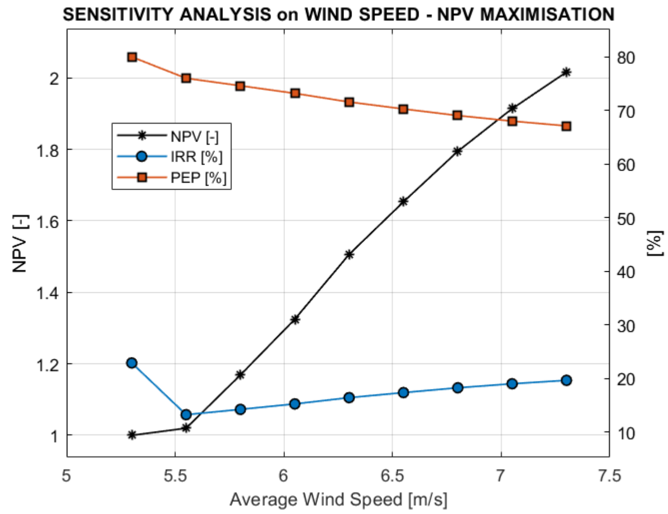

Figure 3.9: Effect of the average wind speed value change on NPV,IRR & PEP
Objective: NPV maximisation - Case study of Iglesias, Italy

Having noted that batteries are never part of the optimal system, a sensitivity analysis on their CAPEX and EoL costs is carried out. The ratio between EoL costs and CAPEX is kept constant and equal to 0.72; a CAPEX reduction of 28% in 15 years is in accordance with the conservative batteries cost projection chosen as a reference [13]. The optimisation is done changing the batteries CAPEX between 100 and 600 €/kWh. Results show how the integration of these devices, regardless of the average electrical load assumed, always causes a decrease in NPV; consequently, they are never part of the optimal system. The reason for this is not to attribute only to the economics of the devices; indeed, simulations previously done show how Iglesias' wind resource is too poor for wind power to be integrated in the most remunerative system. The only-solar system which results the optimal one does not produce enough excess electricity to be stored in batteries. Consequently, their implementation is not meaningful from an economic standpoint.

The procedure is repeated for an average wind speed of 5.8 m/s and an average electrical load of 750 kW, with the objective of seeing what happens in case a fully hybrid HRES is subject to the analysis. Figure 3.10 illustrates the average wind speed at 50 m for the Italian area [14]. A wind source with an average wind speed of 5.8 m/s (yellowish color) is deemed common enough on the territory. The average electrical load follows the results of the analysis previously carried out; the load results to be the minimum for which a DW61-1 MW is part of the most profitable system. No greater loads are chosen for the lower amount of excess electricity available.

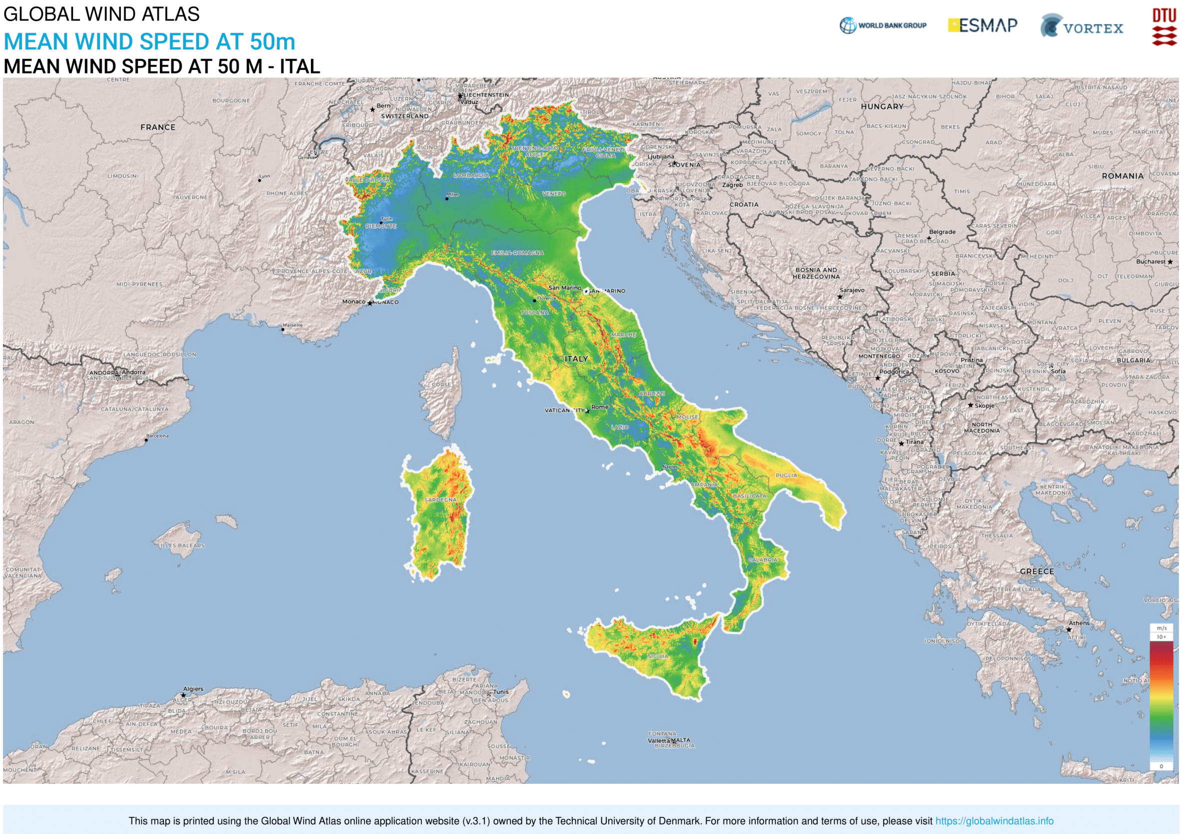

Figure 3.10: Mean wind speed at 50 m of height in Italy

Batteries are integrated in the most remunerative system only for the lowest batteries costs analysed (CAPEX = 100 €/kWh, EoL = 72 €/kWh). The features of the system of interest are displayed in figure 3.3:

Wind Optimal Capacity [kW]	1000
PV Optimal Capacity [kW]	1000
Batteries Optimal Capacity [kWh]	68
PEP [%]	48.25

Table 3.3: Optimised system's main features
u = 5.8 m/s - Average electrical load = 750 kW

The overall outcome of these analysis shows how the integration of batteries in the context of "Renewable Energy Communities" is not advantageous. The characteristics of the incentive structure, that constraints the generation devices' nominal capacity to 1 MW while encouraging the alignment of production and consumption profiles, limit the amount of excess electricity available. Furthermore, the costs of batteries result to be still to high to make these devices attractive for this application.

3.6. Results & Sensitivity Analysis - NPV Maximisation with Negative Externalities -

As stated in section 2.2.2, negative emissions-related externalities linked to the consumption of grid electricity are quantified and considered in the economic performance. To do so, the carbon intensity of the Italian national grid in year 2020, equal to 0.00019 t CO_2eq/kWh [15] is multiplied by the amount of electricity purchased from the grid and by a carbon tax value. When considering the lifetime of the HRES, the carbon footprint is reduced by a constant 4.5% a year to account for the energy mix decarbonisation. The number reflects the scenario of a deep decarbonisation process, where the transition reduces the emissions to 3% of 1990 levels in 2050 [16]. The tax value is shifted in the interval from 30 to 100 €/t CO_2eq. Referring to a stable, constant carbon tax is preferred to considering the EU Emissions Trading Scheme (ETS); indeed, the price of carbon permits is highly volatile and dependent also on macro-economics factors other than the CO2 cap reduction. For this reason, the carbon permits price is difficult to foresee and above all unlikely to stay constant for a time period comparable with a HRES lifetime. Figure 3.11 shows the carbon permits average value since the introduction of the ETS (the unit of measurement of the y axis is €/tCO_2eq).

Figure 3.11: Carbon permits average price in the EU ETS
Source: tradingeconomics.com

Accounting for negative externalities, given the real wind conditions in Iglesias, does not lead to any change in the optimal system design. The most rewarding system stays indeed an only-solar 1 MWp system. Figure 3.12 graphically illustrates the impact of a carbon tax on the system's NPV, given different average electrical loads ranging from 250 to 1000 kW. The value is normalised with respect to the one obtained when neglecting negative externalities and considering an average load of 250 kW. Firstly, the relative NPV for the case of a mean load of 250 kW, being minor than 1, shows how the carbon tax has a negative impact on the system's economic performance. More precisely, the relative NPV oscillates between 0.967 (correspondent to a carbon tax of 30 €/tCO_2eq) to 0.890 (100 €/tCO_2eq). The main reason is to attribute to the expenses carried out to purchase electricity from the grid, while the impact of the PV modules' eco-costs is limited. For instance, in the case of an average electrical load of 250 kW and a carbon tax of 30 €/tCO_2eq, an extra 745'200 € over the whole project lifetime is paid to acquire grid electricity, while only 16'914 € is linked to GHG emissions in the PV module's life-cycle. While the latter value stays constant regardless of the mean load value, the former grows with it; this is due to the linear relationship between the costs sustained and the amount of electricity purchased from the grid. It is described in section 3.5 how, in case of a 1 MWp only-solar system, the NPV reaches its maximum for a mean electrical value of 750 kW and stays constant with larger loads. At the contrary, when accounting for emissions-related externalities, the NPV has a twofold relation with the load magnitude. Whenever the mean load is lower than 625 kW, the benefits taken by an increased self-consumption (and revenues from the incentive) are greater than the economic disadvantages linked to the purchase of a growing amount of electricity from the grid. Consequently, the NPV grows with the load profile's magnitude. The maximum relative NPV (equal to 1.4) is indeed obtained for a mean load of 625 kW. Whenever the mean load is greater than this value, the weight of purchasing electricity overcomes the benefits coming from the incentive and the relative NPV starts decreasing. Furthermore, the greater the mean load, the bigger the impact of the carbon tax value. For instance, for the case with a mean load value of 250 kW, with a carbon tax of 100 €/tCO_2eq the NPV decreases by 7.7% if compared with the situation with a tax equal to 30 €/tCO_2. If the average load value equals 1000 kW, the same increase causes a relative dip in NPV equal to 36.96%. This, which can be noticed by the difference in the graph steepness, is attributable to the greater amount of electricity to be purchased from the grid.

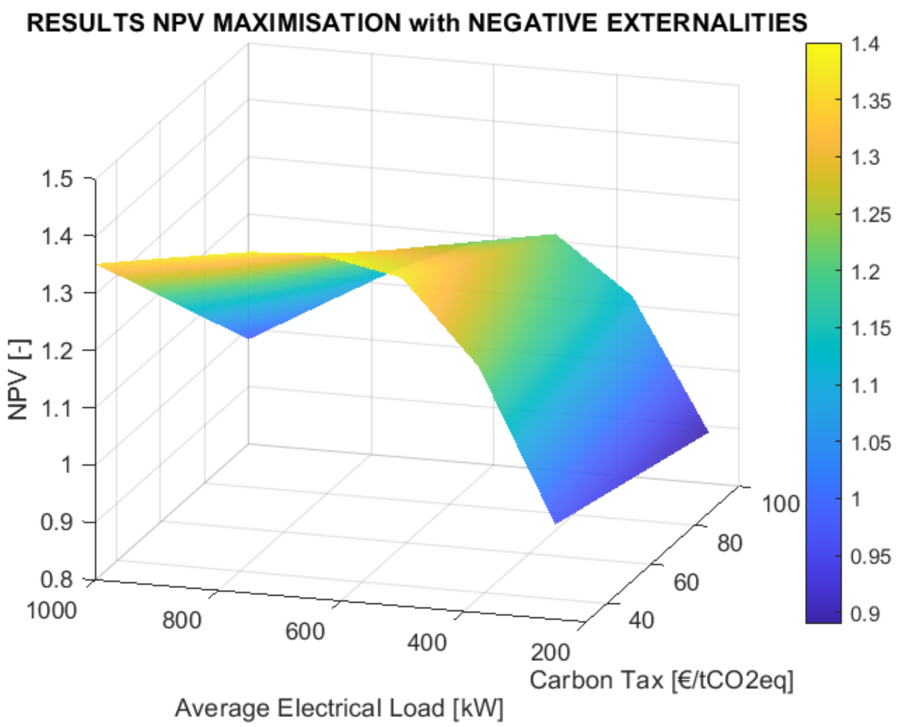

Figure 3.12: Effect of the carbon tax and average electrical load value on the relative NPV of the optimised system
Objective: NPV maximisation - Case study of Iglesias, Italy

The performed analysis suggests how, for a grid-connected HRES located in an area with a poor wind resource and having its nominal installed capacity constrained to target a certain consumers type, a carbon tax spoils the economic performance. However, it must be reminded how a higher carbon tax would have consequences on the decarbonisation pace and, consequently, on the carbon footprint of grid electricity. A more accurate approach would thus consider a correlation between the two.

Additionally, a sensitivity analysis on the wind velocity and carbon tax is conducted. The objective was, as done while neglecting emissions-related externalities, to understand for which conditions a DW61-1 MW is integrated in the optimal system. With u the average wind speed:

- u $\leq$ 5.55 m/s: the most profitable system is an only-solar one for every average load value.
- u $\geq$ 5.55 m/s: wind power starts to get integrated into the system, with a DW61-1 MW wind turbine part of the optimised value for a mean load of at least 750 kW and a minimum carbon tax of 100 €/tCO_2eq.
- u $\geq$ 6.8 m/s: a DW61-1 MW wind turbine is part of the optimised system, regardless of the load and carbon tax characteristics.

In figure 3.13 a comparison between the minimum and optimum average load value when accounting and not for eco costs is displayed. It can be seen how the implementation of a carbon tax makes the installation of a wind turbine attractive for lower loads. The reason is to attribute to the ratio between the additional expenses to carry out when accounting for CO2 emissions. In case of a carbon tax of 30 €/tCO_2eq, for instance, an additional 19'636 € must be paid to install the wind turbine. When considering a mean wind velocity of 5.8 m/s and a mean load of 750 kW (conditions for which a DW61-1 MW is part of the most profitable system with a carbon tax of 30 €/tCO_2eq), the cost of purchasing grid electricity is 101'550 €. Being that the ratio of additional costs is so favourable for the wind turbine, its implementation has a double advantage. The first one lies in the increased revenues stream from the incentive structure, while the second one in the reduction of the costs linked to grid electricity. Consequently, the installation of a DW61-1 MW becomes profitable for higher LCOEs (from 0.046 to 0.047 €/kWh for the aforementioned case). Additionally, as already noticed for only-solar systems, the optimal load lowers with respect to the one obtained when neglecting negative externalities. In that case, indeed, the optimal load is the one which guarantees all the electricity produced to be self-consumed. When accounting for negative externalities, grid electricity comes with an additional cost; a lower load, although it reduces the renewable electricity which is self-consumed, is accompanied by a significant reduction in the amount of electricity to purchase and it thus turns out to be beneficial for the HRES's economic performance.

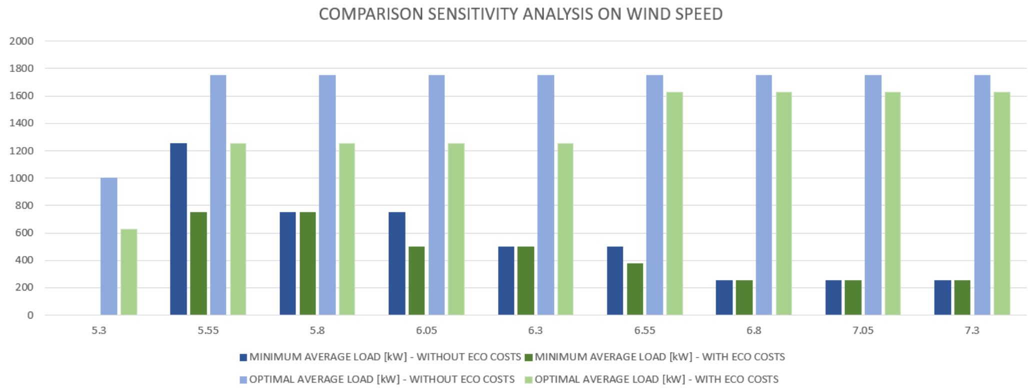

Figure 3.13: Minimum average load to have a DW61-1 MW wind turbine in the optimised system and average load that maximises the economic performance for different average wind velocities. The data is displayed for both the cases when accounting for and neglecting GHG-related negative externalities - Case study of Iglesias, Italy

A sensitivity analysis on the carbon tax value is performed given a mean wind velocity of 5.8 m/s, with the objective of verifying if any remarkable difference in the economic performance of the system is noticeable with respect to the only-solar system. The wind resource is chosen because considered common enough on the Italian territory (see 3.10 for further reference). Similarly to what done for that case, different mean electrical loads, ranging from 250 kW to 1750 kW, are tested. Figure 3.14 illustrates the results of the implemented analysis, in which the NPV is normalised with respect to the one obtained when neglecting negative externalities and considering an average load of 250 kW. The overall surface pattern confirms what previously assessed. The carbon tax has indeed a detrimental effect on the relative NPV; furthermore, it follows a parabolic pattern with respect to the average electrical load. However, the integration of a DW61-1 MW, happening for a mean load of 750 kW, stops the downward trajectory of the surface typical of an only-solar system. Additionally, the maximum relative NPV, equal to 1.5 and obtained for a mean load of 1125 kW, results greater than the one obtained for an only-solar system.

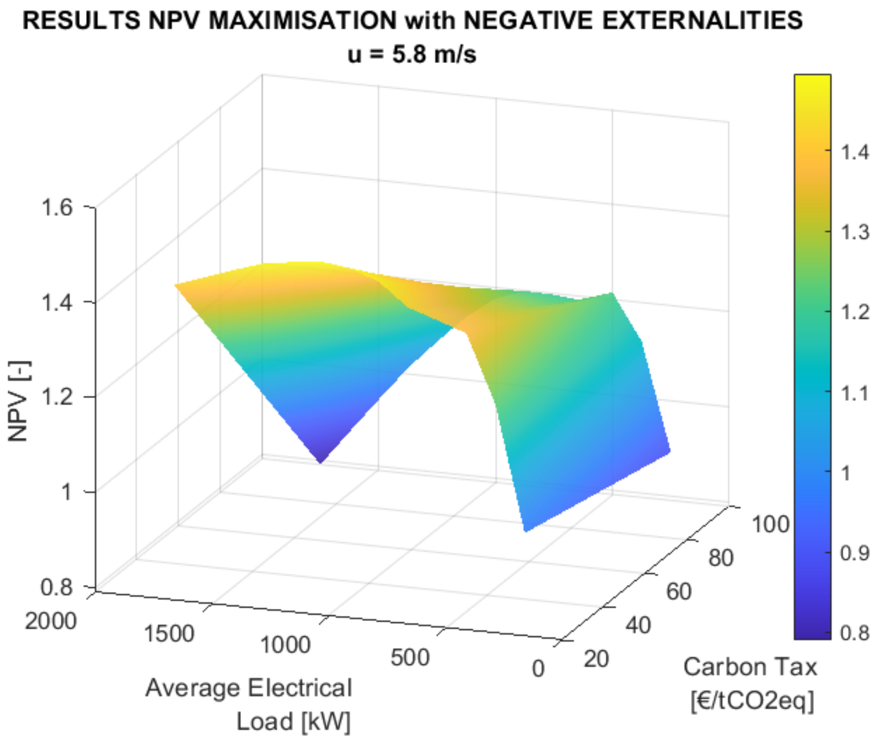

Figure 3.14: Effect of the carbon tax and average electrical load value on the relative NPV of the optimised system given a mean wind speed of 5.8 m/s
Objective: NPV maximisation - Case study of Iglesias, Italy

The results of the performed analysis suggest how the dip in economic performance, measured in most cases when implementing a carbon tax, is attributable to the constraint on installed capacity, rather than to the carbon tax itself. Indeed, as noticed from the sensitivity analysis on the wind source carried out, a tax on GHG emissions accelerates the deployment of renewable energy devices, which become economically attractive for a lower amount of electricity produced. The introduction of a carbon tax, if accompanied by a relaxation of the constraints on the nominal capacity installed, could thus have beneficial effects. Firstly, the optimal renewable capacity, given the same environmental conditions, would be likely to grow; secondly, the NPV of the optimised HRES could increase, leading to larger profits for producers. Lastly, a growth in the installed nominal capacity would be accompanied by an increase in the optimal average load, widening the audience of users part of ”Renewable Energy Communities” and relying on clean energy.

3.7. Results & Sensitivity Analysis - System Independence Maximisation

When the objective function aims to maximise the system independence, the optimiser chases the minimisation of the electricity purchased from the grid. With this aim, the algorithm works to reduce the PEP (see definition from equation 3.1). The lower the PEP, the less electricity the community has to purchase from the grid, being it provided by the HRES installed. Two non-linear constraints are applied: one chains the system’s NPV to be at least equal to zero. The second one constraints the batteries installed to be fully used; consequently, the maximum value of the SOC must be one.

Figure 3.15 shows the results of the optimisation. The system that minimises the PEP is hybrid and made of production devices whose nominal capacity is almost always equal to the maximum allowed (1000 kW for both wind and PV nominal capacity). The only case for which the PV nominal capacity differs from 1000 kW is indeed that with an average load value of 250 kW. Furthermore, when the focus is on the system reliability and not on the economic performance, batteries are part of the mix. It can be seen how a growth in the average electrical load value is accompanied by a dip in the installed batteries' size; this happens because the greater the average electrical load, the less excess electricity is produced. Indeed, all the electricity is self-consumed and nothing can be sent to batteries. Obviously, a bigger electrical load translates into a higher PEP, due to the maximum allowed capacity and constraint on NPV.

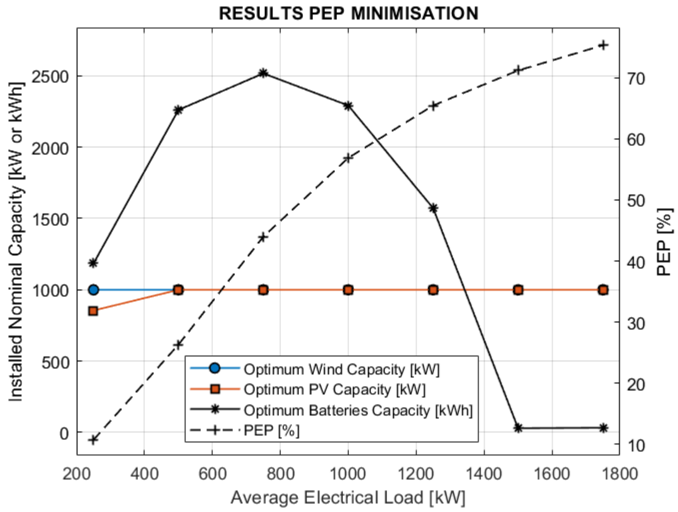

Figure 3.15: Effect of the average load value change on the system size and PEP Objective: PEP minimisation - Case study of Iglesias, Italy

The same sensitivity analysis on wind speed as when maximising the NPV is performed, changing its average value from 5.3 to 7.3 m/s. Figure 3.16 shows the impact of a changing average wind speed on the batteries' optimum capacity and load division, in the case of an average load value of 250 kW. The load is chosen because it guarantees the lowest purchased electricity. The greater the average wind velocity, the more the excess electricity that, instead of being sold to the grid, can be stored. As a consequence, bigger batteries are part of the system. Furthermore, as already noticed when maximising the NPV (see 3.5), the stronger the wind profile, the bigger the percentage of the industrial load profile in the overall demand pattern.

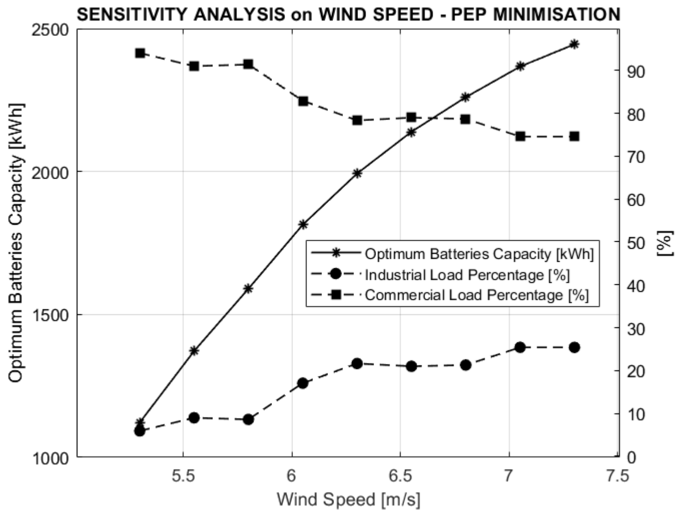

Figure 3.16: Effect of the average wind speed value change on the batteries' optimum capacity and load division Objective: PEP Minimisation - Case study of Iglesias, Italy

Figure 3.17 shows the impact of a changing average wind speed on the techno-economic parameters used to evaluate the system performance. The NPV is always equal to zero as well as the IRR is equal to the real discount rate (in the performed optimisations, 5.88%) due to the constraint applied, that translates into a limit on the system size. As expected, a better wind resource is accompanied by a lower PEP, which, in the best case, decreases until 3.5%. As already mentioned, this effect is attributable to the increased electricity production from the wind turbine.

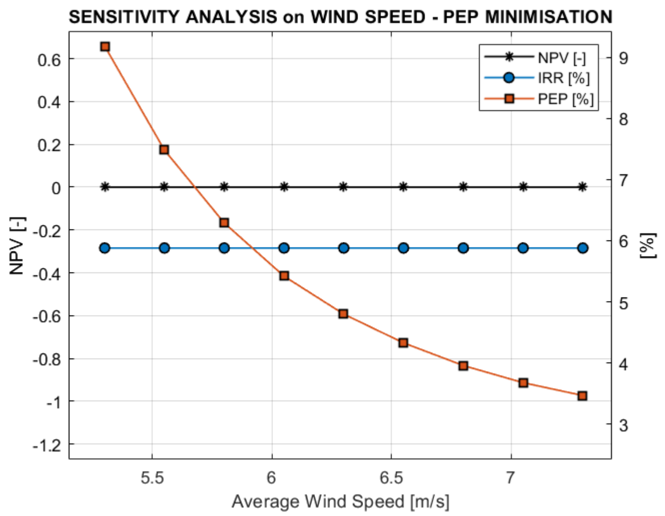

Figure 3.17: Effect of the average wind speed value change on NPV,IRR & PEP Objective: PEP Minimisation - Case study of Iglesias, Italy

4

Use Case 2: Autonomous Systems

This chapter provides the necessary insights about the second of the chosen use cases. Section 4.1 gives an overview of it, with the main characteristics and reasons the use case has been chosen for. Section 4.2 describes the optimisation procedure, defining the variables subject to the process as well as depicting the simulation of the system's functioning. Section 4.3 displays the environmental data used to compute the devices' power production while section 4.4 illustrates the assumed investments to carry out to implement and maintain the HRES. Finally, section 4.5, 4.6 and 4.7 illustrates the results of the performed optimisation and sensitivity analysis for every optimisation objective.

4.1. Use Case Description

The use-case of interest is located in Chumikan, a small town in the far-east of Russia. Picture 4.1 shows its position on the map.

Figure 4.1: Position of Chumikan, Russian Federation

This use-case is representative of an autonomous HRES, located in a remote area. A fish farm, whose yearly electrical demand equals 8.99 GWh, currently relies on a diesel generator, which is subject to a constraint on the minimum power output, equal to 500 kW in the specific case. Figure 4.2 shows the ratio between the minimum generator's output and the needed electrical load.

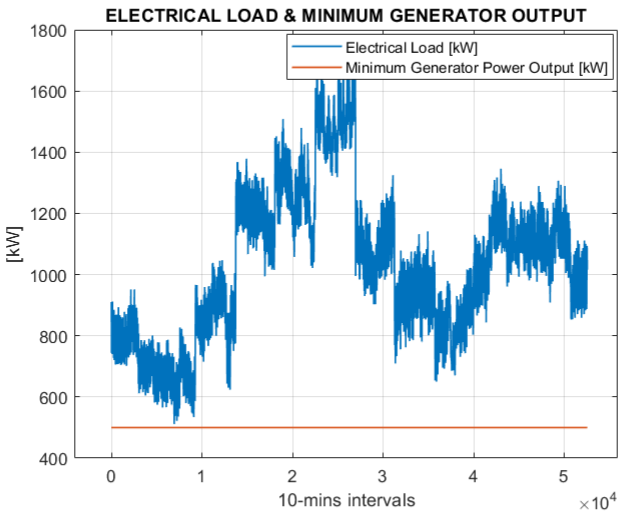

Figure 4.2: Electrical load and minimum generator power output - Case study of Chumikan, Russian Federation

The code also offers the opportunity of setting a different minimum generator power output for each simulated time step; this could be of particular interest whenever the fossil-based device serve different loads but the HRES is planned to serve only one of them. In this case indeed, the generator power output serving the load of interest would depend also on the pattern of the other loads. Homer Pro's way of managing the generator is quite stiff, with a minimum power output always constant in time. Furthermore, this use case is attractive for EWT's business perspective. For these reasons, this case study is considered interesting

4.2. Optimisation

The variables subject to optimisation are the following:

- x_1 : nominal wind capacity [kW];
- x_2 : nominal PV capacity [kW];
- x_3 : nominal batteries energy capacity [kWh];

Each optimisation variable is normalised with respect to the difference between the respective upper and lower limit, for the optimiser to be faster and more precise. For this reason, each variable is bounded between 0 and 1.

The flowchart in figure 4.3 schematically illustrates one iteration of the optimisation process; the decision variables can be found in the green parallelograms while the blue ones contain fixed required inputs.

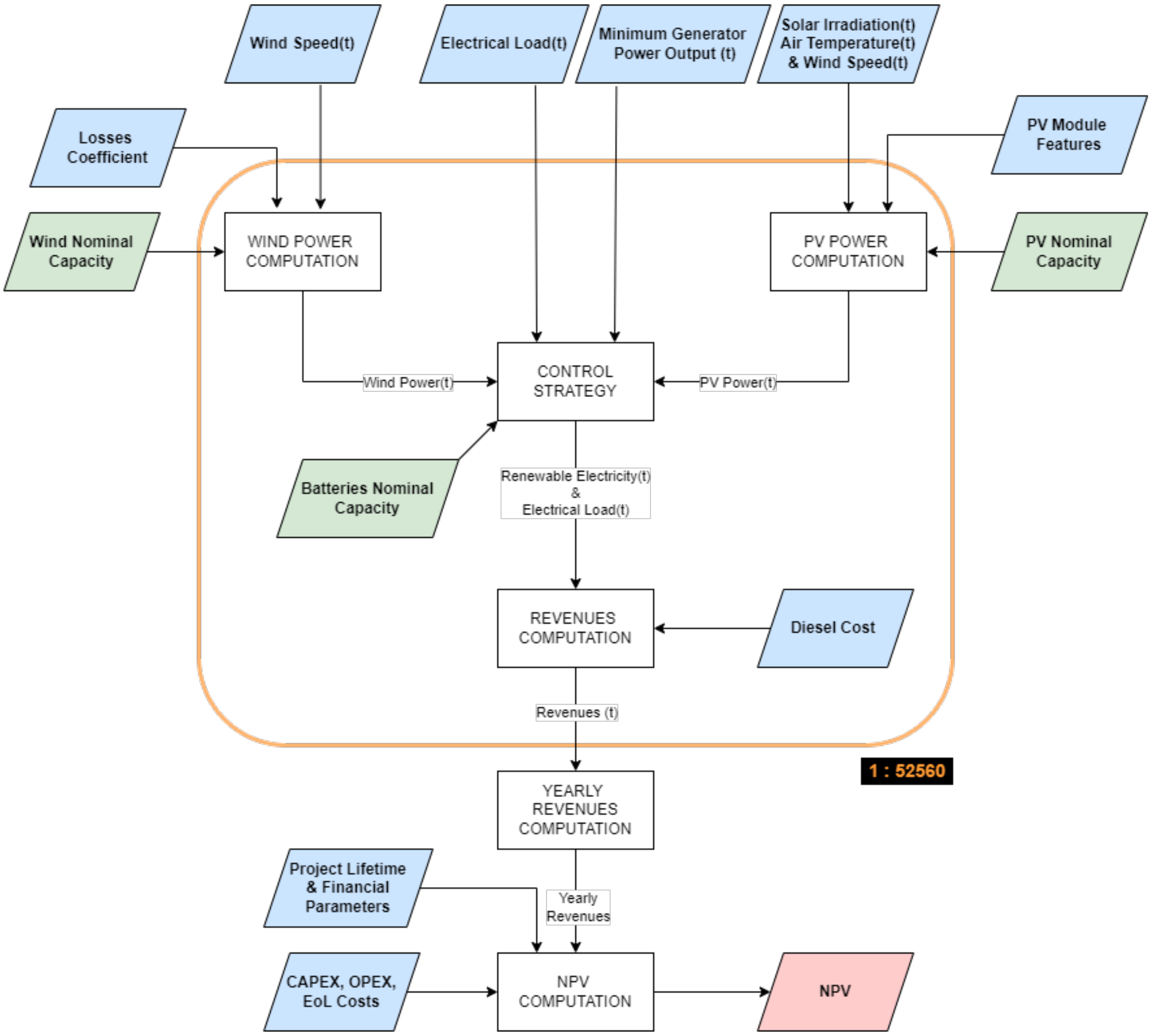

Figure 4.3: Schematic representation of one iteration of the optimisation process - Case study of Chumikan, Russian Federation

Starting from the environmental conditions, the optimiser computes the wind and PV energy production at a certain time step (see 2.3.1 and 2.3.2 for a detailed description of these computations). In the *CONTROL STRATEGY* block, the algorithm establishes the direction of different electricity flows, starting from the comparison between the electricity produced and the demanded one, while heeding the minimum generator power output. The controller has the objective of minimising the Diesel use, while respecting the constraint on its minimum power output. Its value is subsequently subtracted from the electrical load at the time step of interest and the obtained result compared with the renewable production. In case of an overproduction of renewable electricity, the same is sent to the batteries; this priority order is chosen to make the system the most resilient to drops of renewable energy production and, consequently, to limit as much as possible the use of Diesel in time of lack of renewable electricity. The same check is done whenever the minimum generator electricity output is greater than the load. If, due to either the energy or power limit (see 2.3.3), no electricity can be stored in batteries, the remaining energy is curtailed. In case of an underproduction of renewable electricity, the algorithm checks the availability of stored energy in batteries and, applying the energy and power limits (see 2.3.3), determines if the load can be satisfied with it. If it cannot, the generator ramps up to meet the load. As a following step, the revenues at the time step of interest, equal to the savings made by avoiding to burn Diesel and producing electricity through free renewable devices, are calculated through the following equation:

$$R(t) = DC_i \cdot E(t) \tag{4.1}$$

where:

- *R(t)* refers to the revenues at the time interval *t* [€];
- DC_i indicates the Diesel Cost at the year *i* [€/kWh];
- *E(t)* is the electricity matched through free renewable energy [€]

The blocks in the orange square are repeated for each simulated time step (52'560 times in case the chosen interval duration is 10 minutes). The outcome is a scalar representing the revenues in one year of functioning of the system. Given the interest rate charged by investors for loans and the inflation rate, the yearly revenues are actualised for each year falling into the expected project lifetime (equal to 20 years in the performed optimisation). When the same is done with the costs, an actualised cash flow is obtained for each year of the project lifetime. Consequently, the NPV is computed (see 2.2.1 for further details about the performed calculations).

The aforementioned procedure shows how the algorithm determines the NPV for one combination of variables subject to the optimisation. As explained in 2.1, if the conditions for convergence are not respected, the algorithm repeats the process for different values of these variables. The iterations stop whenever the conditions for convergence are respected.

4.3. Environmental Data

This section briefly describes the environmental data used to compute the devices' power production.

4.3.1. Wind Resource

The wind speed time series at each 10 minutes interval is provided by EWT. The correspondent Weibull distribution is described through scale and shape parameters of, respectively, 6.2449 and 1.8537, while the average wind velocity at hub height (46 m) is equal to 5.59 m/s. The capacity factor of a hypothetical DW61 - 1 MW results equal to 24.38%.

4.3.2. Solar Resource & Air temperature

The global irradiance hitting the optimally tilted (52°) module and the air temperature data are downloaded from Meteonorm's database [17]; in more detail, not having meteo stations and thus direct measurements for the desired location, the one of Petropavlosk is chosen. The choice is deemed reasonable, seeing the difference in latitude of only 0.85°and in longitude of 23.15°. The overall irradiation hitting the device in one year is 1488.35 kWh/m^2. Figure 4.4 shows the module temperature during one year of work.

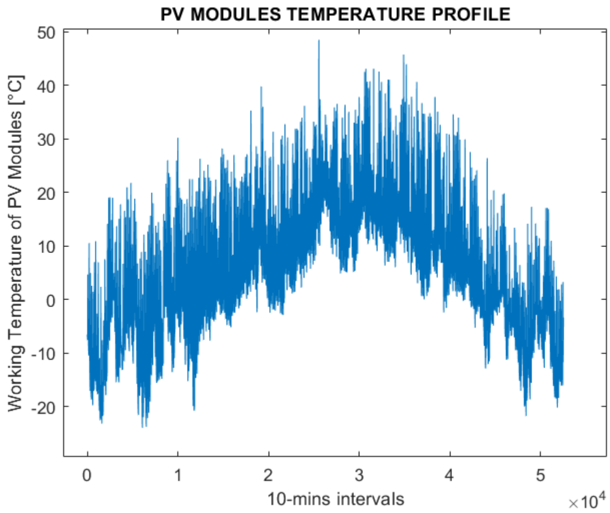

Figure 4.4: Working temperature profile of PV modules in one year of functioning - Case study of Chumikan, Russian Federation

The environmental conditions the PV modules are exposed to in Chumikanm make their average working temperature equal to 5.56 °C. The maximum and minimum working temperatures are, respectively, 48.42 °C and -24 °C. The low minimum temperature does not represent an issue, being the minimum permitted temperature on continuous duty equal to -40°C (see A.1). Figure 4.5 shows the power output profile opposed to the irradiance hitting the optimally tilted module and the relation between the two. The combination of available irradiation and module temperature cause the greatest module power output to be, on average, in spring months.

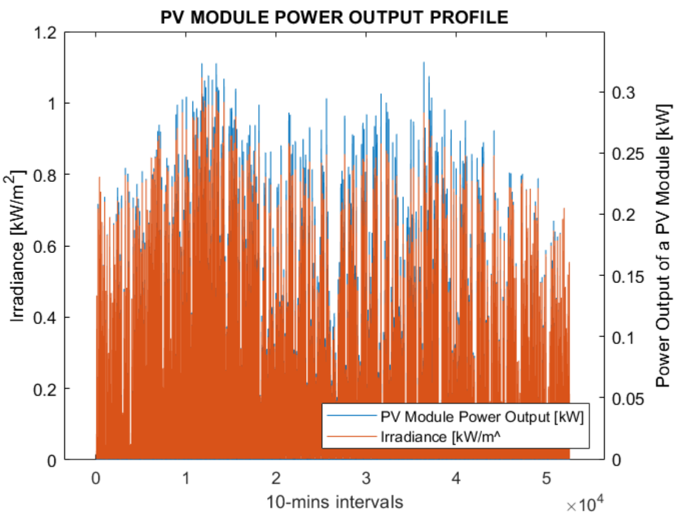

Figure 4.5: Power output of a Hanwha Q.PLUS BFR-G4.1 during one year of functioning and irradiance hitting the optimally tilted module - Case study of Chumikan, Russian Federation

The module's capacity factor results to be 16.78%.

4.4. Costs

This section reports the CAPEX,OPEX and Eol costs used to account for the investments carried out to make and maintain the system.

4.4.1. Wind Power Costs

CAPEX,OPEX and EoL costs of wind turbines are provided by EWT and they are subject to non-disclosure agreement. It is however interesting to notice how the installation of a wind turbine in a remote area such as Chumikan involves an increase in costs. This can be attributed to higher expenses related to transportation of people, materials and turbine installation. Figure 4.6 shows a relative comparison between the wind turbine related costs of the two use cases.

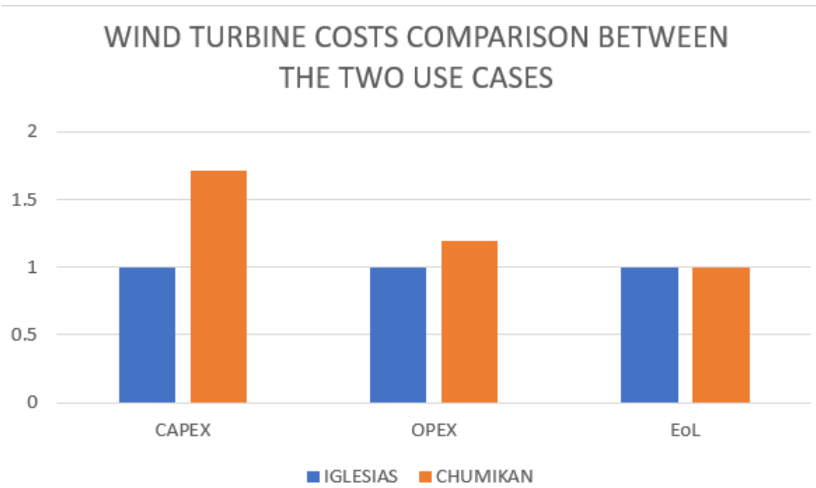

Figure 4.6: Relative comparison between the wind turbine related costs in the two analysed use cases

4.4.2. PV Power Costs

Figure 4.7 shows the average overall CAPEX for PV modules installed in utility-scale systems according to [10]. Not having access to information about the overall cost of distributed PV systems, the utility scale related one is assumed to be representative enough of the real situation. The reported 1889 \$/kWp (≈ 1650 €/kWh) is used. The OPEX is retrieved from the value used for the Italian use-case and the ratio between its respective CAPEX and EoL costs, and it is equal to 15.5 €/kWp. 2020's average costs are preferred to 2021's, because thought to be more representative of a future situation, as they ignore the volatility that occurred in 2021 due to supply chain complications and rising commodity prices [11]. The reported costs include the expenses for the converter.

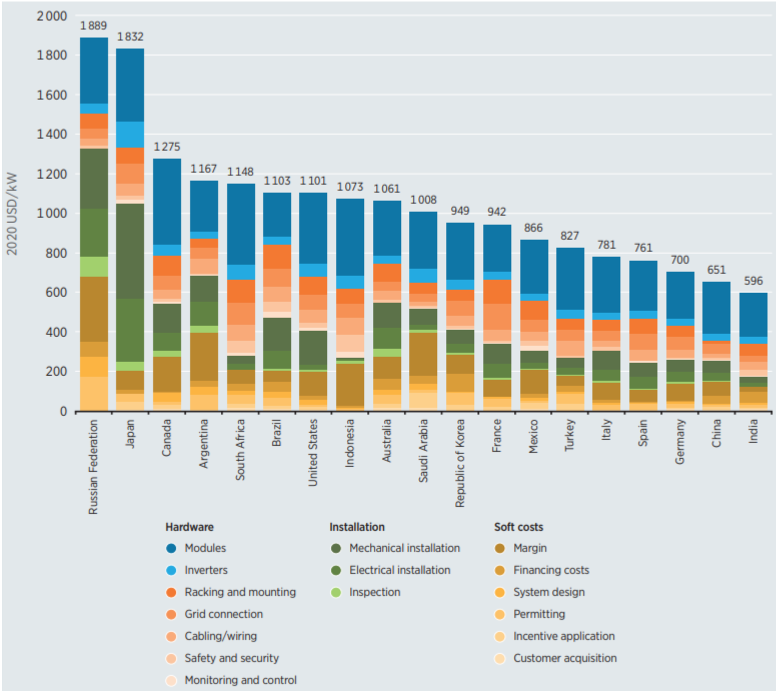

Figure 4.7: Overall CAPEX for utility-scale PV systems
Source: IRENA renewable cost database

4.4.3. Energy Storage Costs

The batteries' costs are assumed, in accordance with EWT, to be equal to those used in the Italian use-case (see 3.4.3). Furthermore, the reported costs include the expenses for the needed inverter.

4.4.4. Generator & Diesel Costs

Being the generator already there and not financed by EWT, CAPEX, OPEX and EoL costs are considered null. The diesel cost is assumed to initially be 0.19 €/kWh, to grow in the following years with a yearly rate of 3.74% [source:EWT].

4.5. Results & Sensitivity Analysis - NPV Maximisation

For the described use-case of Chumikan, the HRES that maximises the NPV is a wind + solar hybrid system, whose main features are resumed in table 4.1, where DEP stands for Diesel Electricity Percentage and indicates the load percentage matched through the diesel generator production, calculated through the following equation:

$$DEP = \frac{E_{diesel}}{L_{total}} \tag{4.2}$$

where:

- E_{diesel} indicates the yearly load matched by using the diesel generator [kWh]
- L_{total} is the annual electrical load [kWh]

Wind Optimal Capacity [kW]	1000
PV Optimal Capacity [kW]	587
Batteries Optimal Capacity [kWh]	0
DEP [%]	75.09
IRR [%]	11.99

Table 4.1: Optimised System's main features - Case study of Chumikan, Russian Federation

Taking advantage of both the solar and wind resource lets the system match a greater part of the load and thus maximise the economic gain.

A sensitivity analysis on the mean wind speed is carried out with the interest of analysing the consequences on the optimised system design. To do so, the wind velocity pattern is adapted changing the average wind velocity from 5.59 to 7.3 m/s. The interval falls into the limits for a class III wind turbine, made to stand a maximum average wind speed of 7.5 m/s. Again, figure 4.8 shows how the growth in the average wind speed value is accompanied by a decrease in the installed PV nominal capacity. Indeed, a better wind resource causes an increase in the wind turbine's capacity factor, which produces more electricity for the same cost. A reduction in the PV nominal capacity represents a reduction in the costs sustained for the same electricity supplied, and thus an increase in NPV.

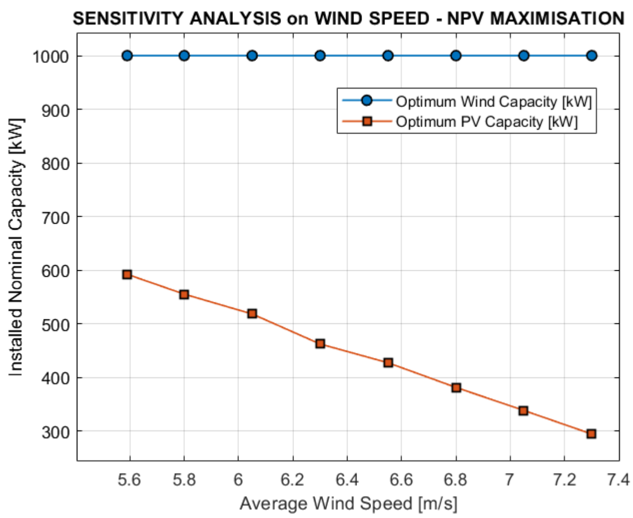

Figure 4.8: Effect of the average wind speed value change on the system size
Objective: NPV maximisation - Case study of Chumikan, Russian Federation

Figure 4.9 shows how the economic parameters are affected by the changing average wind speed. As expected, the higher the average wind speed value, the bigger the NPV and IRR, while the lower the DEP (see 4.7). The greatest percentage reduction in the Diesel generator use results equal to 30% with respect to the current situation.

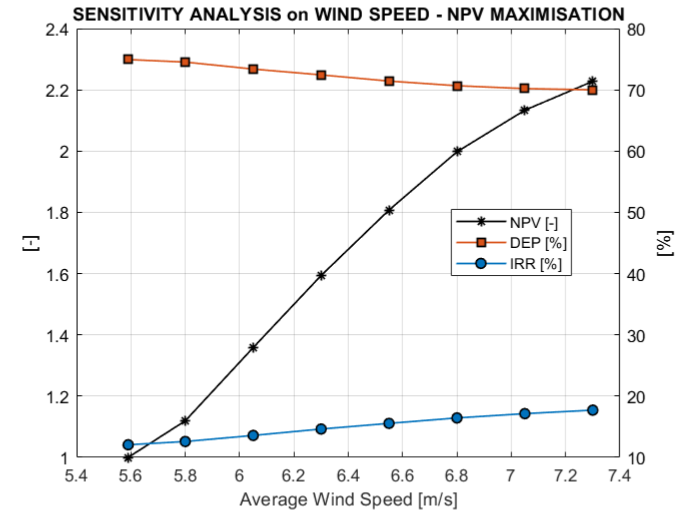

Figure 4.9: Effect of the average wind speed value change on NPV, IRR & DEP
Objective: NPV maximisation - Case study of Chumikan, Russian Federation

Having noted that batteries are never part of the optimal system, a sensitivity analysis on the batteries CAPEX and EoL costs is carried out with respect to the real use case. The ratio between EoL costs and CAPEX is kept constant and equal to 0.72; a CAPEX reduction of 28% in 15 years is in accordance with the conservative batteries cost projection chosen as a reference [13]. The optimisation is done changing the batteries CAPEX between 100 and 600 €/kWh. Figure 4.10 illustrates the results of the analysis. A CAPEX of 350 €/kWh and a consequent EoL cost of 252 €/kWh are the maximum costs for which batteries start getting integrated into the optimal system. With the lowest analysed CAPEX of 100 €/kWh, 1277 kWh of batteries are part of the most remunerative system and take the DEP to 71.25%.

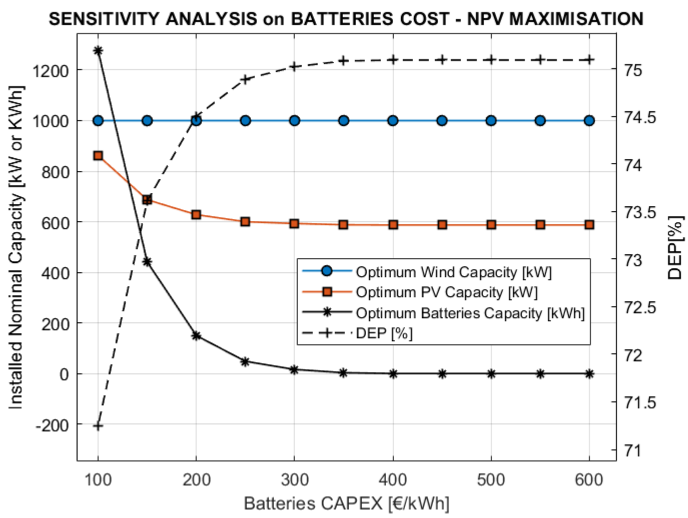

Figure 4.10: Effect of the batteries cost change on the system design and DEP
Objective: NPV maximisation - Case study of Chumikan, Russian Federation

Furthermore, an additional sensitivity analysis is carried out with the scope of understanding how the Diesel cost influenced the optimised system's features. The value ranges from 0.19 to 0.49 €/kWh. The analysis followed an economic interest of EWT after the surge in

Diesel cost recorded in March 2022, after Russian invasion of Ukraine. As shown in figure 4.11, whenever the Diesel cost in year 1 is higher than 0.25 €/kWh, a storage device becomes part of the optimised system. An increase in the Diesel cost indeed makes more attractive to substitute the electricity production from the Diesel generator with that made through renewable devices. This is the reason why a higher Diesel cost is accompanied by an increase in the optimum installed HRES capacity and by a consequent drop of DEP.

It is interesting to notice also how the optimal size of the turbine stays equal to 1 MW regardless of the diesel cost. In other words, it is never convenient to install more than one wind turbine. This can be explained by looking at the LCOE of each device. While the cost for an additional kWh of solar energy is equal to 0.0667 €/kWh, the same kWh of wind energy costs 0.09 €/kWh. When there are no limits on nominal capacity and each kWh is worth the same (that in this case means that each additional kWh matches the load), opting for the technology with the lowest LCOE is always the most meaningful choice.

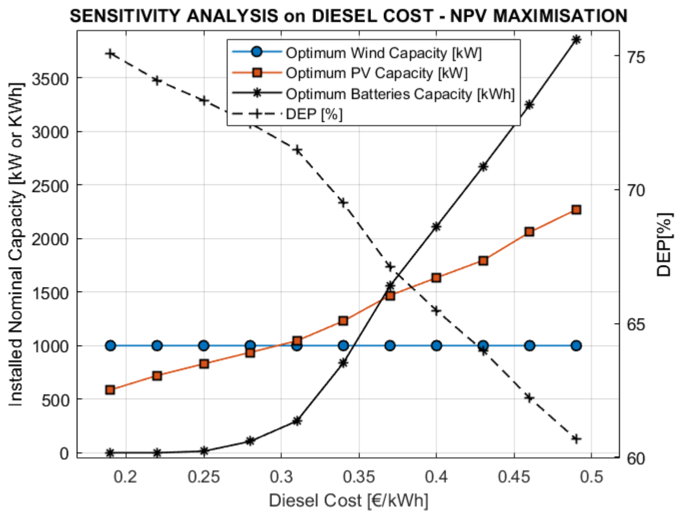

Figure 4.11: Effect of the Diesel cost change on the system design and DEP Objective: NPV maximisation - Case study of Chumikan, Russian Federation

Given the current state of the batteries market, these devices are not economically feasible when considered in a context of a diesel-based HRES. External influences on the market in the forms of remunerative policies to foster the installation of batteries, carbon tax and/or reduction of subsidies towards fossil fuels could make this technology more economically appealing for this application.

4.6. Results & Sensitivity Analysis - NPV Maximisation with Negative Externalities

As anticipated in section 2.2.2, negative emissions-related externalities are, in this case, accounted. For the Diesel generator, a relative approach is carried on; being that the machine is already installed, no additional eco-costs related to its manufacture and EoL are considered. However, the direct GHG emissions caused by the use of the generator is accounted, implementing a carbon tax which translates into a higher Diesel cost (equal to 0.19 €/kWh in the base case). Equation 4.3 resumes the procedure followed:

$$DC = \frac{CT \cdot CF}{1000 \cdot LHV} \tag{4.3}$$

where:

- DC indicates the Diesel Cost [€ / kWh]. The value is obtained summing up the base case price and the additional fraction given by the consideration of a carbon tax.
- CT stands for Carbon Tax and indicates the amount to pay for each unit of CO_2 emitted [€/tCO_2eq]
- Cf is the brief for Carbon Footprint and refers to the mass of CO_2 emitted for each unit of diesel burnt. In the simulations carried out, this value is assumed equal to 3.69 [kgCO_2eq / kgDiesel] (source: HOMER Pro's database)
- LHV is the fuel's Lower Heating Value, equal to 12 kWh / kgDiesel (source:Homer Pro's database)
- 1000 is the number of kgs in a tonne [kg/t]

A sensitivity analysis on the carbon tax value is carried out with the aim of understanding how the nominal capacity of renewable and conventional generation devices is influenced. Its value is modified from 30 to 100 €/tCO_2eq; consequently, the diesel cost is changed in the interval from 0.190 to 0.221 €/kWh.

Figure 4.12 shows how the change in carbon tax value influences the optimal system design. As in case negative externalities are neglected, it's never convenient to install more than one turbine. As mentioned in section 4.5, the reason is to attribute to the difference in LCOE of the different technologies. When the nominal capacity which can be installed is not constrained and each kWh is worth the same, opting for the technology with the lowest LCOE is always the most meaningful choice. The application of a carbon tax does not change the scenario; indeed, the wind turbine's carbon-related additional expenses represent only a tiny part of the overall costs (65'452 € over the whole project lifetime in case of a carbon tax equal to 100 €/t CO_2 eq). For the same conditions, the additional cost paid to account for GHG emissions linked to the lifetime of the PV modules results equal to only 3.4% of the module CAPEX (56'379 € over the whole project lifetime). Consequently, the introduction of a carbon tax is more impactful on the emissions of the Diesel generator. As a results of these two factors combined, the optimal PV capacity increases with respect to the base case. Coherently with what previously found (see section 3.5), being the Diesel cost lower than 0.25 €/kWh also when considering the highest carbon tax, batteries are not integrated in the most rewarding HRES. Furthermore, the grown attractiveness of renewable energy translates into a reduction of the Diesel generator use. Consequently, the DEP decreases by, at most, 0.7% with respect to the base use case until reaching a value of 74.24%.

Figure 4.12 shows how a carbon tax on both direct and indirect emissions affects the system's economic performance. The NPV, here normalised with respect to the one obtained when neglecting negative externalities, grows for greater values of the carbon tax. This is explained by the rise of avoided costs (revenues) linked to the use of free renewable energy rather than diesel made.

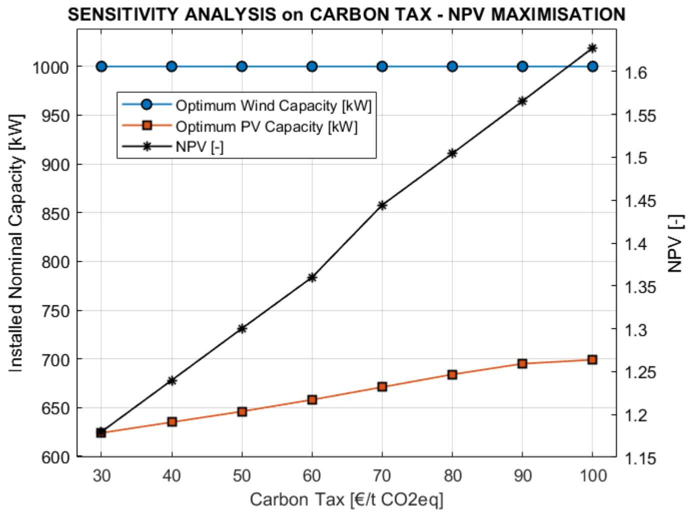

Figure 4.12: Effect of the carbon tax change on the system design and NPV
Objective: NPV maximisation - Case study of Chumikan, Russian Federation

In the case of an autonomous HRES subject to the environmental conditions of Chumikan, the implementation of a carbon tax fosters the installation of renewable energy and improve the economic performance of the optimised system.

4.7. Results & Sensitivity Analysis - System Independence Maximisation

When the objective function aims to maximise the system independence, the optimiser chases the minimisation of the DEP. Two non-linear constraints are applied to respectively bound the minimum allowed NPV to zero and to assure the batteries are fully used (and thus the maximum SOC value is equal to 1). The system which minimises the diesel use is a full hybrid system, whose features are displayed in table 4.2. The optimal system's overall nominal capacity results to be 3 times greater than that obtained when aiming to maximise the revenues.

Wind Optimal Capacity [kW]	1000
PV Optimal Capacity [kW]	1613
Batteries Optimal Capacity [kWh]	2116
DEP [%]	65.25

Table 4.2: Optimised System's Main Features - Case study of Chumikan, Russian Federation

In a similar way to what is done when the aim was to maximise the NPV, a sensitivity analysis on the average wind speed is carried out. Figure 4.13 illustrates the effect of a changing average wind speed value on the system size and DEP. For the whole set of optimised systems, the NPV is equal to zero and thus, the IRR is equal to the real discount rate. The figure shows how, while the wind nominal capacity stay equal to 1 MW, the PV and batteries' nominal capacity grow with a greater average wind speed value. The reason is the same as when maximising the NPV; a better wind resource leads to a greater capacity factor for the wind turbine, which produces more electricity for the same cost. This creates an economic margin which can be spent on additional solar and batteries capacity. As a consequence, the DEP decreases until reaching 58.20%. A further reduction in the use of the diesel generator could be reached only with a NPV lower than zero.

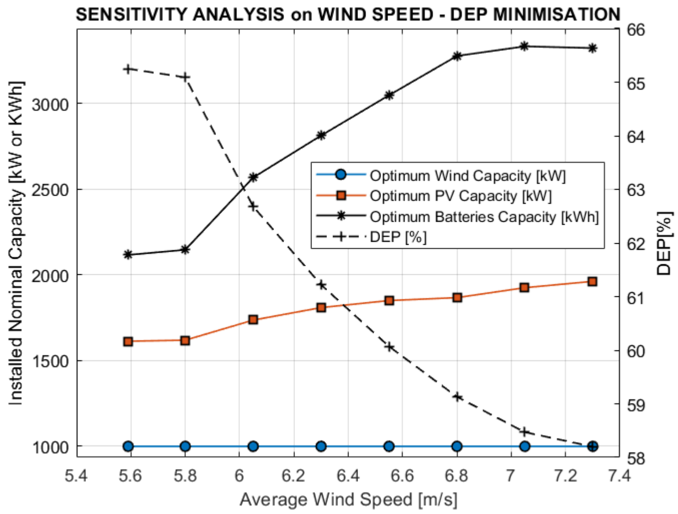

Figure 4.13: Effect of the average wind speed value change on the system size and DEP Objective: DEP minimisation - Case study of Chumikan, Russian Federation

Following the sensitivity analysis on the batteries and Diesel cost done when the optimisation aims to maximise the NPV, an additional simulation considering the most favourable conditions is carried out. Given a diesel cost of 0.49 €/kWh, a battery CAPEX of 100 €/kWh and an EoL cost of 72 €/kWh, the optimised system size results to be the following:

Wind Optimal Capacity [kW]	2000
PV Optimal Capacity [kW]	6937
Batteries Optimal Capacity [kWh]	52900
DEP [%]	47.73

Table 4.3: Optimised System's Main Features - Case study of Chumikan, Russian Federation

Can be noticed how the optimal system still relies on the Diesel generator to match almost half of the electrical load. A further reduction of DEP would need the removal of the constraint to keep a positive NPV. This outcome shows how, even in the most favourable economic conditions, the full substitution of fossil-based generators in case of large loads disconnected from the grid, and not exposed to exceptional weather conditions, results to be challenging. However, wind turbines with a greater nominal capacity, taking advantage of economies of scale, could improve the scenario.

5

Validation

This chapter provides an overview about how the written codes are validated. Section 5.1 illustrates the process for the first of the chosen use cases, while section 5.2 does the same for the second one.

5.1. Validation - Renewable Energy Communities

Seeing the impossibility of optimising the load as well as describing the incentive structure through Homer Pro, a comparison between the results obtained for a given HRES is carried out. With this purpose, a grid-connected wind+solar system located in Iglesias and serving an AC industrial load is modeled. Its mean power request, equal to 250 kW, gives an yearly electrical demand of 2.19 GWh/year. The HRES is made of a DW61-1 MW turbine and Hanwha Q.PLUS BFR-G4.1 modules with an overall nominal capacity of 1 MWp.

The power production profiles result to be accurate. Given the same wind conditions, HOMER PRO returns a capacity factor for the wind turbine of 19.67%, exactly equal to that returned by the made HRES optimisation framework. For what concerns the PV power, Homer Pro returns a capacity factor of 20.9%, that differs from the one obtained with the made framework by a mere 0.59%. The difference is most probably given by the different rationale behind the PV power computation, which in Homer Pro considers only the Global Horizontal Irradiance (GHI), combined with a sky clearness index, neglected in the made HRES optimisation framework. Additionally, the model behind the cell temperature computation is different than the one implemented in the framework. Indeed, the minimum operating cell temperature is, according to Homer Pro, equal to 9.42°C (+8.18°C with respect to the one returned in the performed simulations); the maximum one is instead 56.25°C (-1.11 °C). No mean temperature can be displayed by HOMER PRO.

The system functioning and economics see some more differences in results, seeing the impossibility of modeling in Homer Pro the incentive for self-consumption. For this reason, the value of the incentive is set equal to zero in the simulation performed with the made HRES optimisation framework. This choice makes the system handling differently the various electricity flows. While the made optimisation framework always prioritises the load matching, regardless of the incentive inserted, HOMER PRO prefers to sell the electricity to the grid to make revenues. This is also the reason why batteries are decided not to be part of this validation system. Seeing the absence of a reward for self-consumption as well as the gratuitousness of electricity taken from the grid, energy would have never been sent to the batteries. According to HOMER PRO, the electricity sold to the grid is equal to 2.09 GWh/year (+0.11 GWh/year, +5,56%) while that purchased from the grid is equal to 0.77 GWh/year (+0.06

GWH/year, +8.33%). Finally, HOMER PRO gives a NPV for the described case of -1.78 M€, which overcomes the outcome given by the made optimisation framework by 0.09 M€ (+4.8%). The difference is a consequence of what previously described. Figure 5.1 is a graphical representation of what explained in these lines. Illustrations about the outcomes of Homer Pro can be find in B

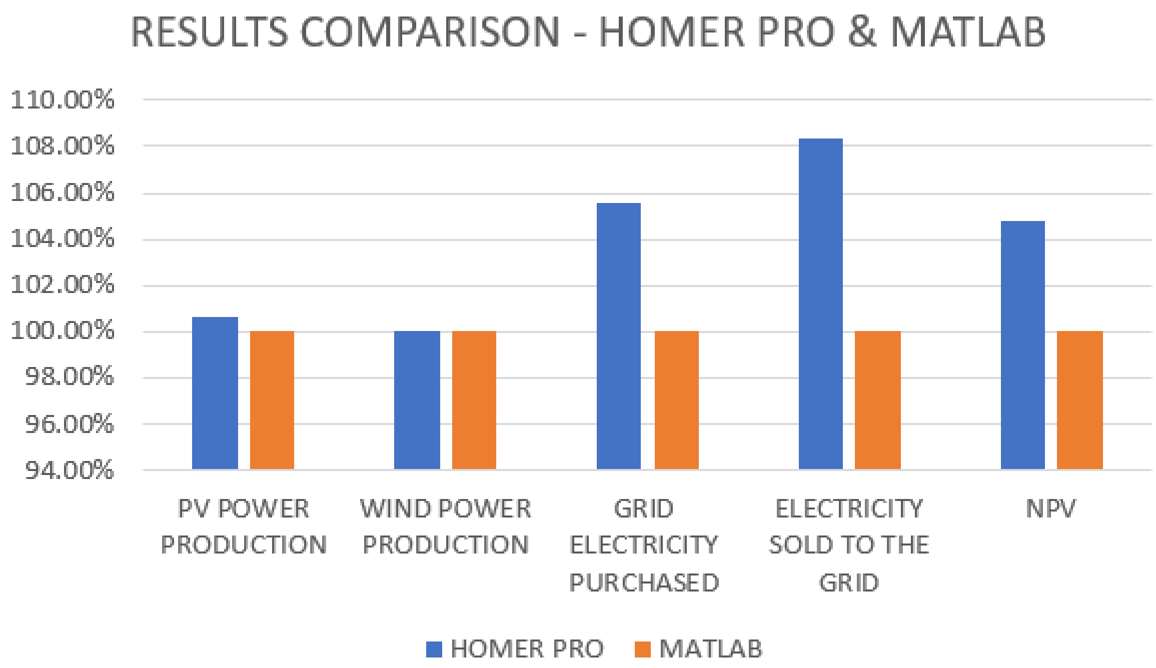

Figure 5.1: Comparison between the results obtained with HOMER PRO and the made optimisation framework (referred to as MATLAB) - Case study of Iglesias, Italy

5.2. Validation - Autonomous Systems

HOMER PRO does not offer the possibility of modeling the savings made by avoiding the use of Diesel in favour of renewable electricity as they were revenues. For this reason, the cash flow would necessarily be different, leading to a different NPV (in HOMER Pro, minus NPC); consequently, the suggested optimised system would be different. For this reason, a comparison between the results obtained for a given HRES is carried out. With this purpose, an autonomous wind+solar+Diesel system located in Chumikan and serving the AC load of interest is modeled. Its mean power request, equal to 1026.2 kW, gives an yearly electrical demand of 8.99 GWh/year. The HRES is made of a DW61-1 MW turbine and Hanwha Q.PLUS BFR-G4.1 modules with an overall nominal capacity of 587 kWp.

The power production profiles result to be accurate. Given the same wind conditions, HOMER PRO returns a capacity factor for the wind turbine of 24.4%, only 0.2% greater than the one returned by the made HRES optimisation framework. This slight difference is probably to attribute to a different approximation of wind velocities not multiple of 0.5 m/s; this leads to a different computation of the wind power produced through the application of the inserted wind power curve for some of the simulated time intervals. For what concerns the PV power, Homer Pro returns a capacity factor of 18.3%, that differs from the one obtained with the made framework by 1.52%. As in the other use case. the difference is most probably given by the different rationale behind the PV power computation, which in Homer Pro considers only the Global Horizontal Irradiance (GHI), combined with a sky clearness index, neglected in the performed simulations. Additionally, the model behind the cell temperature computation is different than the one implemented in the framework. Indeed, the minimum operating cell temperature is, according to Homer Pro, equal to -25,02 (-1.02°C with respect to the one returned by the made optimisation framework); the maximum one is instead 46.07°C (-2.35 °C). No mean temperature can be displayed by HOMER PRO. The generator power output turns out to be 6.74 GWh/year (-0.1 GWh/year, -1.48%).

The same DEP of 75.09% shows how the system functioning modeled is aligned with what displayed by HOMER Pro. On the contrary, the economics parameters do not relate, seeing the different consideration of revenues flow. Figure 5.2 is a graphical representation of what explained in these lines. Illustrations about the outcomes of Homer Pro can be found in B.

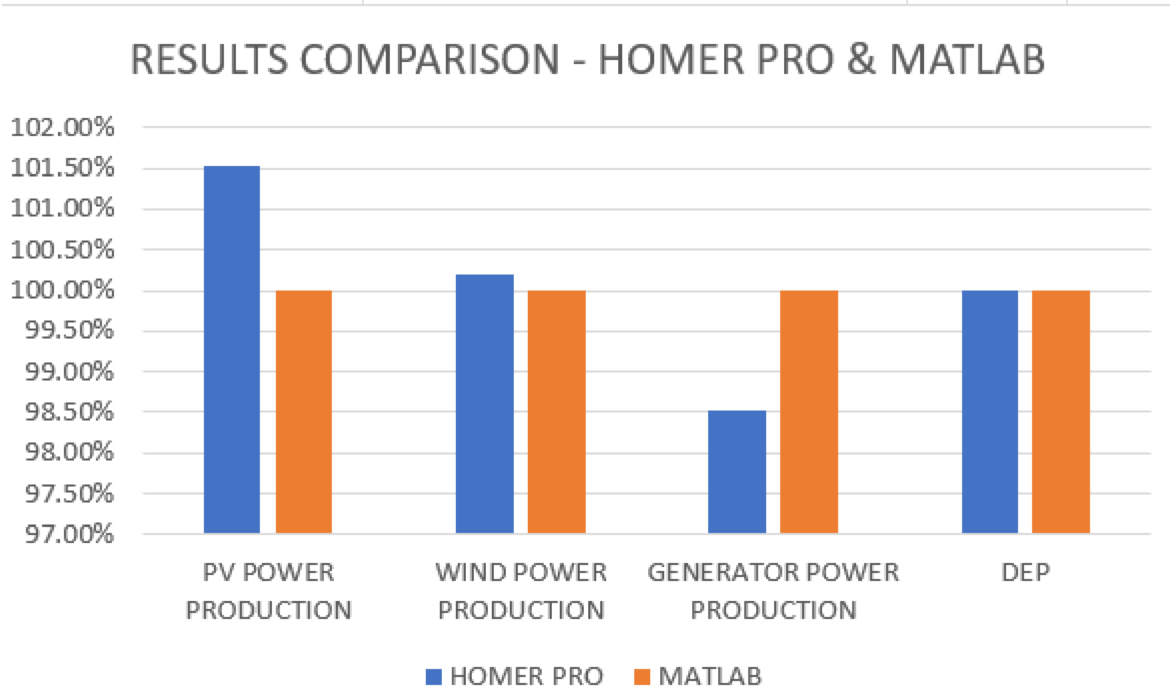

Figure 5.2: Comparison between the results obtained with HOMER PRO and the made optimisation framework (referred to as MATLAB) - Case study of Chumikan, Russian Federation

6 Conclusions

A software to optimally size HRES given different inputs, constraints and objective functions has been implemented and used to run simulations on two different use cases. This chapter provides the reader with the most relevant insights from their analysis:

6.1. Conclusions - Renewable Energy Communities

- When the objective is to maximise the economic performance of the system, relevant parameters are the costs of devices and weather resources availability, that converge in the LCOE. Given the chosen site's weather conditions, wind energy is never part of the most profitable system. The reason is to attribute to poor wind resource, that translates into an LCOE of 0.067 €/kWh, around two and a half times greater than solar's, equal to 0.026 €/kWh. A DW61-1 MW turbine starts to get integrated in the optimised system for an LCOE lower than 0.054 €/kWh. The optimisation outcome is here influenced by the constraint on nominal capacity as well as by the incentive structure. The latter indeed introduces a difference in each kWh's value; specifically, a kWh which is self-consumed is worth more than one that is, for instance, sent to the grid. Consequently, it is more meaningful to install a wind turbine rather than additional cheaper solar panels when the additional electricity produced increases the self consumption enough to maximise the overall profit. Furthermore, once reached the constraint on nominal capacity for an only-solar system, the installation of additional PV modules is prevented and opting for the most expensive technology becomes a necessity.
- When the aim is maximising the economic performance of the HRES, the integration of batteries is not likely to be advantageous. In the context of the Italian "Renewable Energy Communities", indeed, the characteristics of the incentive structure, that constraints the generation devices' nominal capacity to 1 MW while encouraging the alignment of production an consumption profiles, limit the amount of excess electricity available. Furthermore, the costs of batteries result to be still to high to make these devices attractive for this application.
- A carbon tax accelerates the deployment of renewable energy devices, which become economically attractive for higher LCOEs. The reason for that is the growth in additional expenses to carry out when purchasing electricity from the grid. The implementation of a wind turbine has thus a two-fold benefit. The first one lies in the increased revenues stream coming from the incentive structure, while the second one in the reduction of the costs linked to grid electricity. However, a carbon tax should be accompanied by a

parallel relaxation of the constraints on nominal capacity, needed to have beneficial effects on the system's economic performance. Without it, the increase in grid-purchased electricity costs spoils the system's economic performance if compared with the case negative GHG-related externalities are neglected.

- When the objective lies in maximising the system independence, a full hybrid system (wind+solar+storage) is always the best option. However, when the load to serve gets larger, making the system fully independent becomes, from an economic standpoint, problematic. The relaxation of constraints on nominal capacity could change the scenario.

6.2. Conclusions - Autonomous Systems

- Given Chumikan's weather conditions and the objective of maximising the economic performance, the optimised solution sees the integration of solar and wind energy. A wind+solar hybrid system indeed guarantees to match a greater part of the load and leads to the greatest possible economic gain. As the sensitivity analysis performed on the Diesel cost showed how, after a wind turbine is installed, additional capacity tends to be solar, due to a lower LCOE. Indeed, when there are no limits on nominal capacity and each kWh is worth the same (that in this case means that each additional kWh matches the load), opting for the technology with the lowest LCOE is always the most meaningful choice.
- Given the current state of the batteries market, these devices are not economically feasible when considered in a context of a diesel-based HRES. Indeed, results from simulations showed how batteries start to get integrated in the most rewarding system for economic conditions different than the one assumed to be realistic. Indeed, either a diesel cost greater than 0.25 €/kWh or a CAPEX for batteries lower than 350 €/kWh causes the integration of these devices in the optimised HRES. Consequently, external influences on the market in the forms of remunerative policies to foster the installation of batteries, carbon tax and/or reduction of subsidies towards fossil fuels could make this technology more economically appealing for this application.
- In the case of an autonomous HRES not subject to any constraint on nominal capacity, the implementation of a carbon tax always fosters the installation of renewable energy devices and improve the economic performance of the optimised system. This is to attribute to the greater impact of a tax system on diesel generator's direct emissions rather than on those connected to renewable energy.
- When the objective lies in maximising the system's independence, a full hybrid system (wind+solar+batteries) is the best option. However, even in the best economic conditions, the full substitution of fossil-based generators in case of large loads disconnected from the grid, and not exposed to exceptional weather conditions, results to be unprofitable.

Bibliography

[1] S. Sinha and S. Chandel, “Review of software tools for hybrid renewable energy systems,” *Renewable and Sustainable Energy Reviews*, vol. 32, pp. 192–205, 2014.

[2] A. Tummalieh, A. J. Beinert, C. Reichel, M. Mittag, and H. Neuhaus, “Holistic design improvement of the pv module frame: Mechanical, optoelectrical, cost, and life cycle analysis,” *Progress in Photovoltaics: Research and Applications*, 2022.

[3] “Sandia module temperature model,” 2021. https://pvpmc.sandia.gov/modeling-steps/2-dc-module-iv/module-temperature/sandia-module-temperature-model/.

[4] Continental Energy Solutions, “Hybrid power plants - nrel hybrid optimization and performance platform (hopp) | solar podcast ep 81,” 2021. https://www.youtube.com/watch?v=jEI5lRJ$_uCMt = 1984s.$

[5] M. Dwisatyawati, A. Paranjape, A. Reppas, A. Rottigni, and J. Voultsos, “Techno-economic assessment of distributed hybrid renewable energy systems,” 2021.

[6] S. Mudgal, Y. Guern, B. Tinetti, A. Chanoine, S. Pahal, F. Witte, *et al.*, “Comparative life-cycle assessment of nickel-cadmium (nicd) batteries used in cordless power tools (cpts) vs. their alternatives nickel-metal hybride (nimh) and lithium-ion (li-ion) batteries. final report of european commission. bio intelligence service, paris, france,” *Final Report of European Commission. Paris: Bio Intelligence Service*, 2011.

[7] L. da Silva Lima, M. Quartier, A. Buchmayr, D. Sanjuan-Delmás, H. Laget, D. Corbisier, J. Mertens, and J. Dewulf, “Life cycle assessment of lithium-ion batteries and vanadium redox flow batteries-based renewable energy storage systems,” *Sustainable Energy Technologies and Assessments*, vol. 46, p. 101286, 2021.

[8] M. Jaganmohan, “Distribution of solar photovoltaic module production worldwide in 2020, by country,” *Renewable and Sustainable Energy Reviews*, 2022.

[9] European Commission, “Photovoltaic geographical information system,” 2019. https://re.jrc.ec.europa.eu/pvg$_tools/it/MR.$

[10] International RENewable Energy Agency (IRENA), “Renewable power generation costs in 2020,” tech. rep., International Renewable Energy Agency, Abu Dhabi, 2021.

[11] International Energy Agency (IEA), “Renewable electricity market update,” tech. rep., International Energy Agency, Paris, 2021.

[12] Ricerca Sistema Energetico (RSE), “L’accumulo elettrochimico di energia: nuove regole, nuove opportunità,” tech. rep., Ricerca Sistema Energetico, Milan, 2021.

[13] W. Cole, A. W. Frazier, and C. Augustine, “Cost projections for utility-scale battery storage: 2021 update,” tech. rep., National Renewable Energy Lab.(NREL), Golden, CO (United States), 2021.

[14] ENERGYDATA.INFO, “Global wind atlas,” 2022. https://globalwindatlas.info/.

[15] M. R. Hannah Ritchie and P. Rosado, “Energy,” *Our World in Data*, 2020. https://ourworldindata.org/energy.

[16] M.Borasio and S.Moret, “Deep decarbonisation of regional energy systems: A novel modelling approach and its application to the italian energy transition,” *Renewable and Sustainable Energy Reviews*, 2022.

[17] MeteoTest, “Meteonorm,” 2022. https://meteonorm.com/en/.

A

Appendix A

A.1. Sandia Module Temperature Model

Module Type	Module Mount	a	b
Glass/cell/glass	Open rack	-3.47	-0.0594
Glass/cell/glass	Close roof mount	-2.98	-0.0471
Glass/cell/polymer sheet	Open rack	-3.56	-0.0750
Glass/cell/polymer sheet	Insulated Back	-2.81	-0.0455
Polymer/thin-film/steel	Open rack	-3.58	-0.113
22X Linear Concentrator	Tracker	-3.23	-0.130

Table A.1: Temperature coefficients a and b for different module types and mounting configurations Source: [3]

A.2. PV Module Technical Sheet

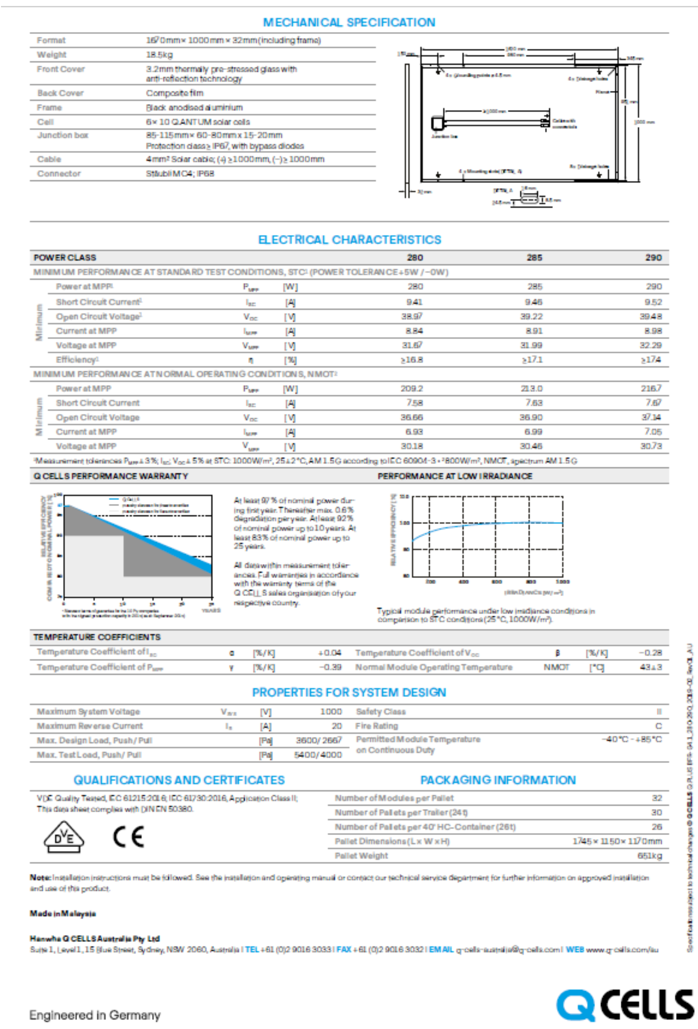

MECHANICAL SPECIFICATION

Format	1670 mm × 1000 mm × 32 mm (including frame)
Weight	18.5 kg
Front Cover	3.2 mm thermally pre-stressed glass with anti-reflection technology
Back Cover	Composite film
Frame	Black anodised aluminium
Cell	6 × 10 QANTUM solar cells
Junction box	85-115 mm × 60-80 mm x 15-20 mm Protection class ≥ IP67, with bypass diodes
Cable	4 mm² Solar cable; (+) ≥ 1000 mm, (−) ≥ 1000 mm
Connector	Stäubli MC4; IP68

ELECTRICAL CHARACTERISTICS

POWER CLASS				280	285	290
MINIMUM PERFORMANCE AT STANDARD TEST CONDITIONS, STC[1] (POWER TOLERANCE +5W / −0W)						
Minimum	Power at MPP[1]	P_{MPP}	[W]	280	285	290
	Short Circuit Current[1]	I_{SC}	[A]	9.41	9.46	9.52
	Open Circuit Voltage[1]	V_{OC}	[V]	38.97	39.22	39.48
	Current at MPP	I_{MPP}	[A]	8.84	8.91	8.98
	Voltage at MPP	V_{MPP}	[V]	31.67	31.99	32.29
	Efficiency[1]	η	[%]	≥16.8	≥17.1	≥17.4
MINIMUM PERFORMANCE AT NORMAL OPERATING CONDITIONS, NMOT[2]						
Minimum	Power at MPP	P_{MPP}	[W]	209.2	213.0	216.7
	Short Circuit Current	I_{SC}	[A]	7.58	7.63	7.67
	Open Circuit Voltage	V_{OC}	[V]	36.66	36.90	37.14
	Current at MPP	I_{MPP}	[A]	6.93	6.99	7.05
	Voltage at MPP	V_{MPP}	[V]	30.18	30.46	30.73

[1]Measurement tolerances P_{MPP} ±3%; I_{SC}; V_{OC} ±5% at STC: 1000 W/m², 25±2 °C, AM 1.5G according to IEC 60904-3 • [2]800 W/m², NMOT, spectrum AM 1.5G

Q CELLS PERFORMANCE WARRANTY

At least 97% of nominal power during first year. Thereafter max. 0.6% degradation per year. At least 92% of nominal power up to 10 years. At least 83% of nominal power up to 25 years.

All data within measurement tolerances. Full warranties in accordance with the warranty terms of the Q CELLS sales organisation of your respective country.

PERFORMANCE AT LOW IRRADIANCE

Typical module performance under low irradiance conditions in comparison to STC conditions (25 °C, 1000 W/m²).

TEMPERATURE COEFFICIENTS

Temperature Coefficient of I_{SC}	α	[%/K]	+0.04	Temperature Coefficient of V_{OC}	β	[%/K]	−0.28
Temperature Coefficient of P_{MPP}	γ	[%/K]	−0.39	Normal Module Operating Temperature	NMOT	[°C]	43±3

PROPERTIES FOR SYSTEM DESIGN

Maximum System Voltage	V_{SYS}	[V]	1000	Safety Class	II
Maximum Reverse Current	I_R	[A]	20	Fire Rating	C
Max. Design Load, Push / Pull		[Pa]	3600 / 2667	Permitted Module Temperature on Continuous Duty	−40 °C - +85 °C
Max. Test Load, Push / Pull		[Pa]	5400 / 4000		

QUALIFICATIONS AND CERTIFICATES

VDE Quality Tested, IEC 61215:2016; IEC 61730:2016, Application Class II; This data sheet complies with DIN EN 50380.

PACKAGING INFORMATION

Number of Modules per Pallet	32
Number of Pallets per Trailer (24 t)	30
Number of Pallets per 40' HC-Container (26 t)	26
Pallet Dimensions (L × W × H)	1745 × 1150 × 1170 mm
Pallet Weight	651 kg

Note: Installation instructions must be followed. See the installation and operating manual or contact our technical service department for further information on approved installation and use of this product.

Made in Malaysia

Hanwha Q CELLS Australia Pty Ltd
Suite 1, Level 1, 15 Blue Street, Sydney, NSW 2060, Australia | TEL +61 (0)2 9016 3033 | FAX +61 (0)2 9016 3032 | EMAIL q-cells-australia@q-cells.com | WEB www.q-cells.com/au

Engineered in Germany

Figure A.1: Hanwha Q.PLUS BFR-G4.1 Technical Sheet
Source: Q Ceels

A.3. Battery Technical Sheet

Technical Datasheet Freqcon MSC 1000 Wind (Hybrid)

Inverter

Manufacturer	FREQCON GmbH
Nominal AC voltage	620 VAC
AC power frequency (nominal)	50 Hz
Maximum apparent power	1100 kVA
Maximum AC current (I)	1024 A
Nominal active power	1000 kW
Power factor at rated power / adjustable	1 / 0.03 overexcited to 0.0 underexcited
Max. Inverter efficiency AC to DC (STC)	98.3%
Max. Inverter efficiency DC to DC (STC)	99.4%
Nominal DC Link voltage	1250 VDC
6-pulse rectifier	2 x 600VDC
Short-circuit current protection (max)	max. 40 kA @ 620 V
Number of DC outputs for Battery	2
DC voltage range	700 VDC to 1022 VDC
DC current per output / DC current combined	2 x 1000 ADC / 2000 ADC
Size of Inverter cabinet	3000 x 2431 x 1200 (W x H x D)
Housing (inverter, battery, HVAC)	40 ft. HC container

Battery Storage

Battery cell	LFP LF280K
Manufacturer	EVE
Battery cells per module	10 (10S)
Battery module	LFP8960
Battery modules per rack	28
Battery cells per rack	280
Battery capacity per rack	250.88 kWh
Number of battery racks	4
BESS capacity (installed)	1,003 kWh
BESS capacity (usable)	900 kWh
Cycles @ 90% DoD | 80% EoL | 25 °C +/- 5 °C 1C / 1C	> 4,000
Battery storage temperature range (> 1 month)	0 °C to 35 °C (30% to 50% SoC)
Ambient temperature range (operation)	-20 °C to 40 °C

Controller

Main Controller	Siemens Simotion P320-4
Control software	FREQCON Framework
Applications	Energy arbitrage, reactive power compensation, Peak Shaving etc.
Response time	< 150 ms
Internal communication	Profinet IRT
External communication interfaces	Ethernet, MODBUS TCP, Profinet
Maximum total harmonic distortion	< 3% at nominal power

Protective Devices and Standards

Battery (DC)	Fuse and DC load break switch
AC side disconnection point	Air circuit breaker
DC overvoltage protection	Surge arrester, type I
AC overvoltage protection	Surge arrester, class I
Ground fault monitoring	Yes
Insulation monitoring	Yes
Protection level	IP54
Fire protection (converter)	Smoke and arc detection
Cooling principle (converter)	Liquid cooled
Maximum permissible value for relative humidity (condensing / non-condensing)	95% to 100% (2 month/year) / 0% to 95%
Inverter Life (rated conditions)	20 years
Battery Life (rated conditions)	10 to 15 years

A.4. Wind Turbine Mass Composition

3 Turbine recycling and disposal overview

Turbine type			Mass [kg]	Percentage of building block mass [%]	Percentage of turbine mass [%]	Recycling / Disposal percentage [%]	Method [-]
DW61-900kW HH69			**545.998**	**-**	**100%**	**-**	**-**
Building Block	**Component**	**Material type**	**-**	**-**	**-**	**-**	**-**
Foundation	-	-	421.422	100%	77,2%	-	-
	Concrete	Concrete, bricks, …etc.	408.012	96,8%	74,7%	64%	Landfill
	Rebar	Carbon steel	9.710	2,3%	1,8%	95%	Recycling
	Anchor	Carbon steel	3.700	0,9%	0,7%	95%	Recycling
Tower	-	-	64.010	100%	11,7%	-	-
	Tower walls & platforms	Carbon steel	62.100	97,0%	11,4%	95%	Recycling
	Entrance steps	Carbon steel	200	0,3%	0,0%	95%	Recycling
	Power & Control cables	Copper, magnesium, nickel, zinc and their alloys	900	1,4%	0,2%	98%	Recycling
		Plastics, rubber and other organic materials	400	0,6%	0,1%	100%	Incineration with energy recovery
	Ladder	Aluminum and aluminum alloys	390	0,6%	0,1%	95%	Recycling

Building Block	Component	Material type	Mass [kg]	Percentage of building block mass [%]	Percentage of turbine mass [%]	Recycling / Disposal percentage [%]	Method [-]
	Lighting & outlets	Electronics (e.g. Elec motors, PLC's, sensors … etc.)	30	0,0%	0,0%	50%	Recycling with energy recovery
Nacelle	-	-	9.965	100	1,8%	-	-
	Nacelle housing	Carbon steel	7.800	78,4%	1,4%	95%	Recycling
	Nacelle cover	Glass Reinforced Epoxy / Polyester	130	1,3%	0,0%	95%	Landfill
	Ladder	Aluminum and aluminum alloys	15	0,2%	0,0%	95%	Recycling
	Grease pump	Carbon steel	10	0,1%	0,0%	95%	Recycling
		Lubricants (oil, grease … etc.)	7	0,1%	0,0%	90%	Recycling
	Hydraulic power pack	Carbon steel	40	0,4%	0,0%	95%	Recycling
		Lubricants (oil, grease … etc.)	5	0,1%	0,0%	90%	Recycling
		Plastics, rubber and other organic materials	4	0,0%	0,0%	100%	Incineration with energy recovery
	Yaw bearing	Low Alloy steel	800	8,0%	0,1%	95%	Recycling
		Lubricants (oil, grease … etc.)	2	0,0%	0,0%	90%	Recycling
	Yaw drive	Low Alloy steel	300	3,0%	0,1%	95%	Recycling
		Cast Iron	450	4,5%	0,1%	95%	Recycling
		Lubricants (oil, grease … etc.)	26	0,3%	0,0%	90%	Recycling
		Electronics (e.g. Elec motors, PLC's, sensors … etc.)	126	1,3%	0,0%	50%	Recycling with energy recovery

Building Block	Component	Material type	Mass [kg]	Percentage of building block mass [%]	Percentage of turbine mass [%]	Recycling / Disposal percentage [%]	Method [-]
	Nacelle controls	Carbon steel	50	0,5%	0,0%	95%	Recycling
		Electronics (e.g. Elec motors, PLC's, sensors … etc.)	120	1,2%	0,0%	50%	Recycling with energy recovery
	Chain hoist	Carbon steel	30	0,3%	0,0%	95%	Recycling
		Electronics (e.g. Elec motors, PLC's, sensors … etc.)	30	0,3%	0,0%	50%	Recycling with energy recovery
	Rescue kit	Plastics, rubber and other organic materials	20	0,2%	0,0%	100%	Incineration with energy recovery
Generator	-	-	30.750	100%	5,6%	-	-
	Stator & Rotor	Carbon steel	15.600	50,7%	2,9%	95%	Recycling
		Low Alloy steel	7.800	25,4%	1,4%	95%	Recycling
		Copper, magnesium, nickel, zinc and their alloys	4.100	13,3%	0,8%	98%	Recycling
		Plastics, rubber and other organic materials	180	0,6%	0,0%	100%	Incineration with energy recovery
	Main Bearing	Low Alloy steel	2.100	6,8%	0,4%	95%	Recycling
		Lubricants (oil, grease … etc.)	15	0,0%	0,0%	90%	Recycling
	Covers	Glass Reinforced Epoxy / Polyester	540	1,8%	0,1%	95%	Landfill

Building Block	Component	Material type	Mass [kg]	Percentage of building block mass [%]	Percentage of turbine mass [%]	Recycling / Disposal percentage [%]	Method [-]
	Power cables	Copper, magnesium, nickel, zinc and their alloys	300	1,0%	0,1%	98%	Recycling
		Platics, rubber and other organic materials	100	0,3%	0,0%	100%	Incineration with energy recovery
	Service brake	Cast Iron	8	0,0%	0,0%	95%	Recycling
		Carbon steel	7	0,0%	0,0%	95%	Recycling
Hub	-	-	9.588	100%	1,8%	-	-
	Hub housing	Cast Iron	6.000	62,6%	1,1%	95%	Recycling
		Carbon steel	300	3,1%	0,1%	95%	Recycling
		Low Alloy steel	45	0,5%	0,0%	95%	Recycling
	Nose Cone	Glass Reinforced Epoxy / Polyester	66	0,7%	0,0%	95%	Landfill
	Pitch drives	Low Alloy steel	38	0,4%	0,0%	95%	Recycling
		Cast Iron	58	0,6%	0,0%	95%	Recycling
		Lubricants (oil, grease … etc.)	2	0,0%	0,0%	90%	Recycling
		Electronics (e.g. Elec motors, PLC's, sensors … etc.)	26	0,3%	0,0%	50%	Recycling with energy recovery

Building Block	Component	Material type	Mass [kg]	Percentage of building block mass [%]	Percentage of turbine mass [%]	Recycling / Disposal percentage [%]	Method [-]
	Pitch bearing	Low Alloy steel	2.700	28,2%	0,5%	95%	Recycling
		Lubricants (oil, grease … etc.)	5	0,1%	0,0%	90%	Recycling
	Hub controls	Carbon steel	134	1,4%	0,0%	95%	Recycling
		Electronics (e.g. Elec motors, PLC's, sensors … etc.)	210	2,2%	0,0%	50%	Recycling with energy recovery
		Batteries	29	0,3%	0,0%	100%	Recycling
	Lightning cables	Copper, magnesium, nickel, zinc and their alloys	3	0,0%	0,0%	98%	Recycling
		Plastics, rubber and other organic materials	1	0,0%	0,0%	100%	Incineration with energy recovery
Blades (3x)	-	-	8.086	100	1,5%	-	-
	Blade body	Glass Reinforced Epoxy / Polyester	7.950	98,3%	1,5%	95%	Landfill
		Low Alloy steel	100	1,2%	0,0%	95%	Recycling
	Lightning cables	Copper, magnesium, nickel, zinc and their alloys	30	0,4%	0,0%	98%	Recycling
	Platform	Wood	6	0,1%	0,0%	90%	Incineration with energy recovery

Building Block	Component	Material type	Mass [kg]	Percentage of building block mass [%]	Percentage of turbine mass [%]	Recycling / Disposal percentage [%]	Method [-]
Converter	-	-	2.267	100%	0,4%	-	-
	Cabinet	Copper, magnesium, nickel, zinc and their alloys	600	26,5%	0,1%	98%	Recycling
		Low Alloy steel	460	20,3%	0,1%	95%	Recycling
		Carbon steel	520	22,9%	0,1%	95%	Recycling
		Electronics (e.g. Elec motors, PLC's, sensors … etc.)	410	18,1%	0,1%	50%	Recycling with energy recovery
	Cooler	Carbon steel	172	7,6%	0,0%	95%	Recycling
		Coolant liquid	55	2,4%	0,0%	100%	Chemical disposal plant
		Plastics, rubber and other organic materials	50	2,2%	0,0%	100%	Incineration with energy recovery

Table 2: Complete overview of turbine component masses and recycling and disposal method percentages.

A.5. Provenience of Wind Turbine's Materials

Generator	China
Converter	Germany
Tower	Italy
Tower Internals	Germany
Blade - Glass Fiber	China
Blade - Epoxies	Germany
Blade - Polymer & rest of materials	Germany, Benelux
Nacelle - Housing & Cover	China
Nacelle - Internals	Italy, Germany, Netherlands
Hub - Housing	China
Hub - Metal Parts	India
Hub - Electrical Components	Germany, Netherlands
Foundation	Denmark, Spain

Table A.2: Provenience of the main components of a DW61-900 kW

A.6. Graphic User Interface

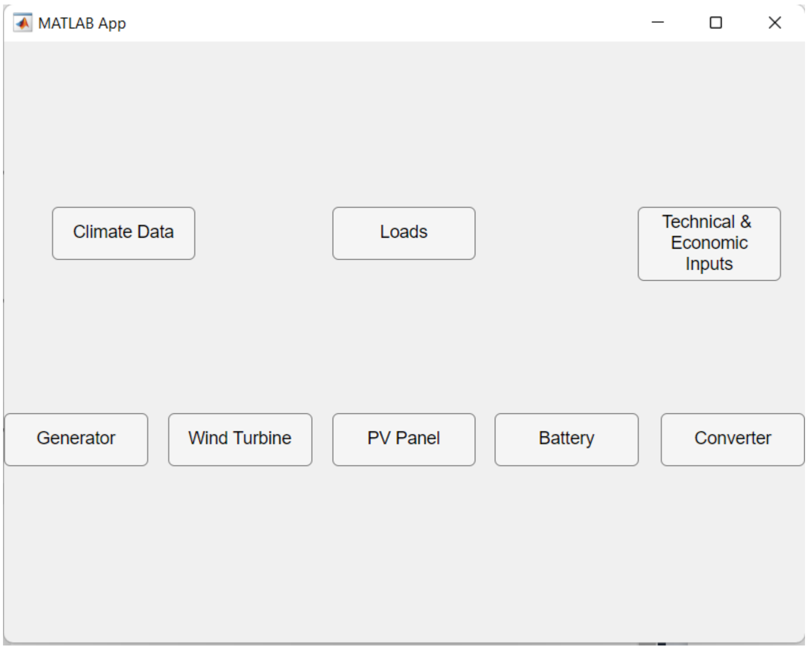

Figure A.2: GUI page 1

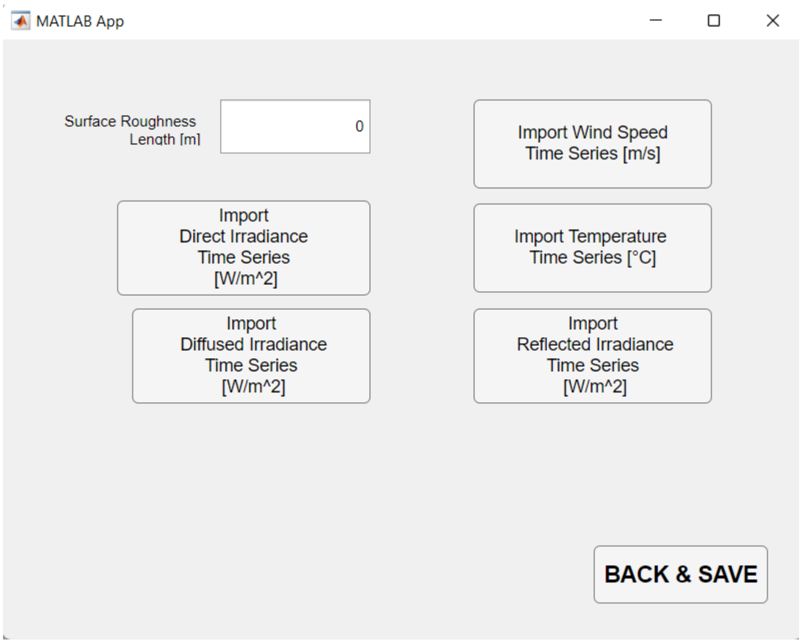

Figure A.3: GUI Climate Data

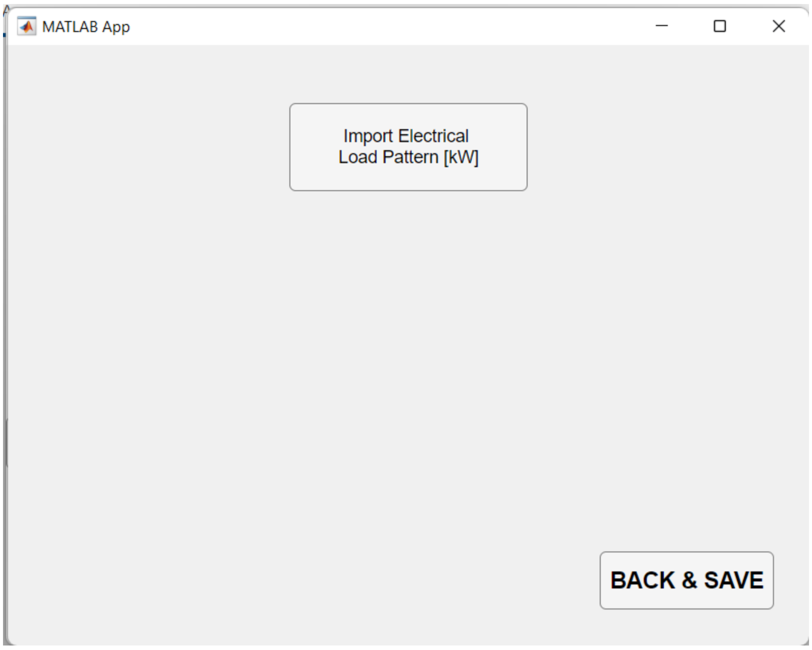

Figure A.4: GUI Loads

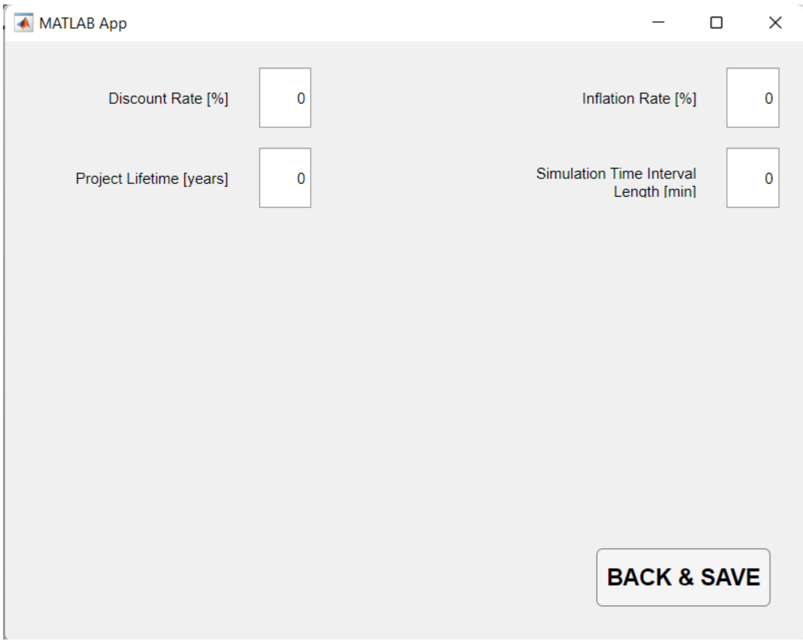

Figure A.5: GUI Technical Economic Inputs

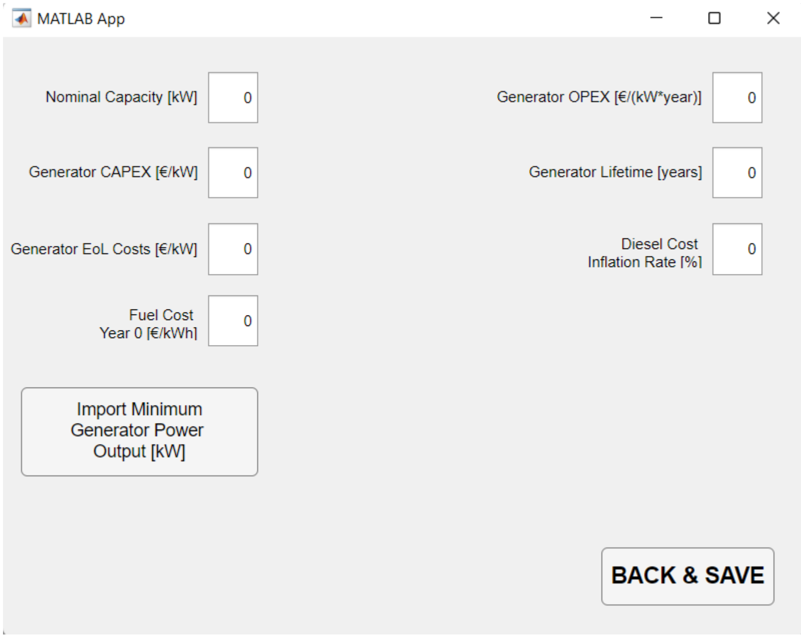

Figure A.6: GUI Generator

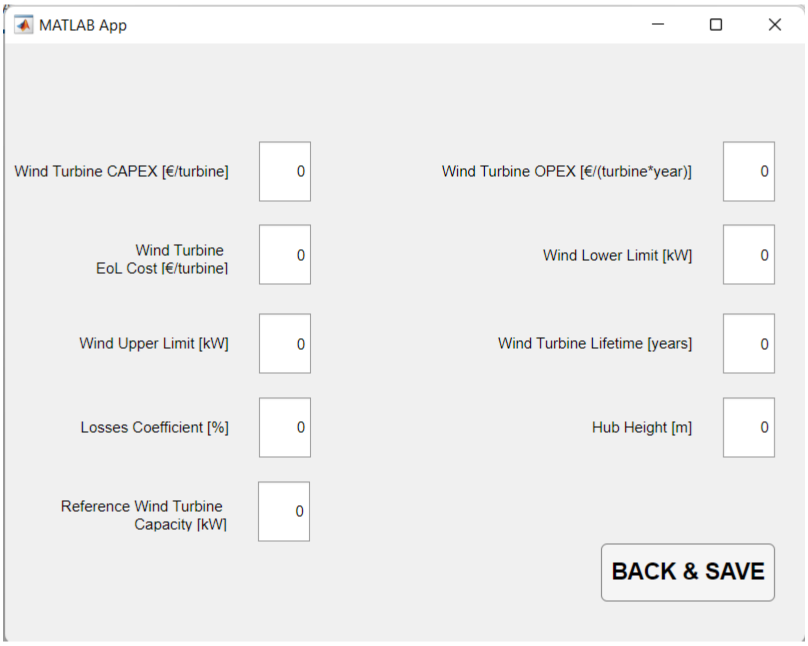

Figure A.7: GUI Wind Turbine

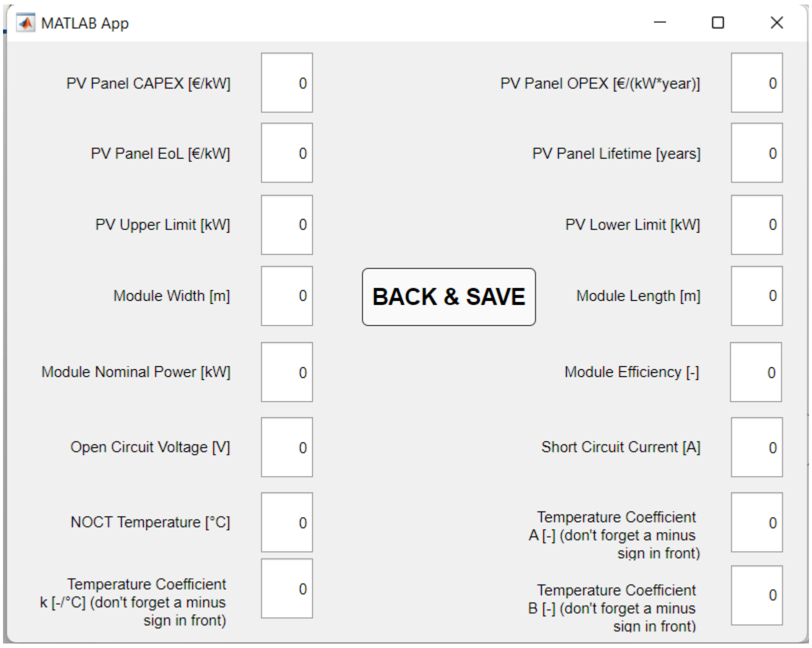

Figure A.8: GUI PV Panel

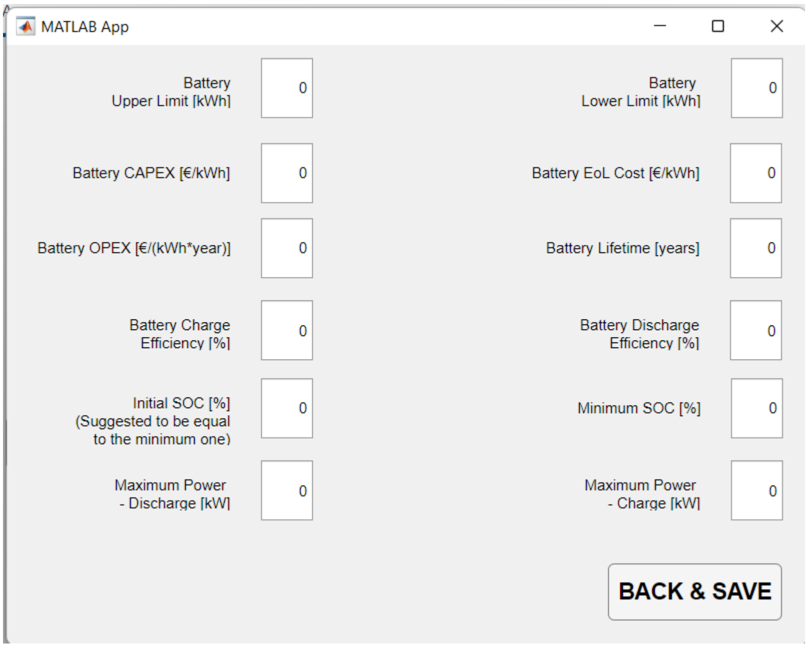

Figure A.9: GUI Battery

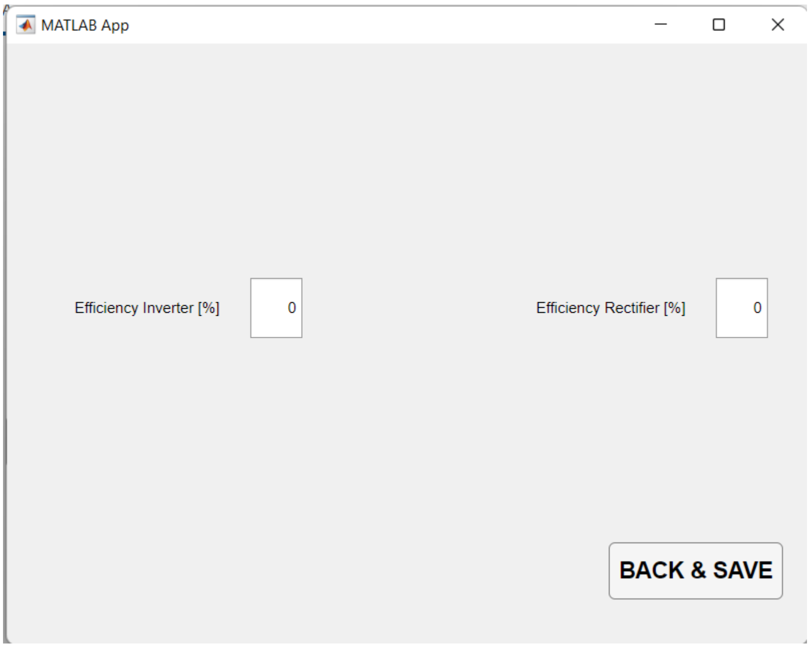

Figure A.10: GUI Converter

B

Appendix B - Validation with Homer Pro

B.1. Electrical Load - Renewable Energy Communities

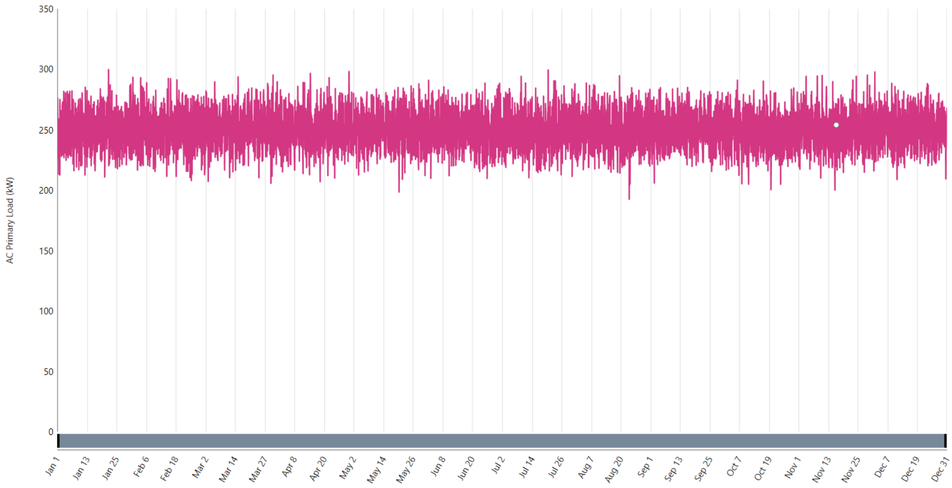

Figure B.1: Electrical load yearly pattern

B.2. PV Modules Power Production - Renewable Energy Communities

Quantity	Value	Units
Rated Capacity	1,000	kW
Mean Output	209	kW
Mean Output	5,027	kWh/d
Capacity Factor	20.9	%
Total Production	1,834,981	kWh/yr

Quantity	Value	Units
Minimum Output	0	kW
Maximum Output	1,100	kW
PV Penetration	83.8	%
Hours of Operation	4,385	hrs/yr
Levelized Cost	0.0448	€/kWh

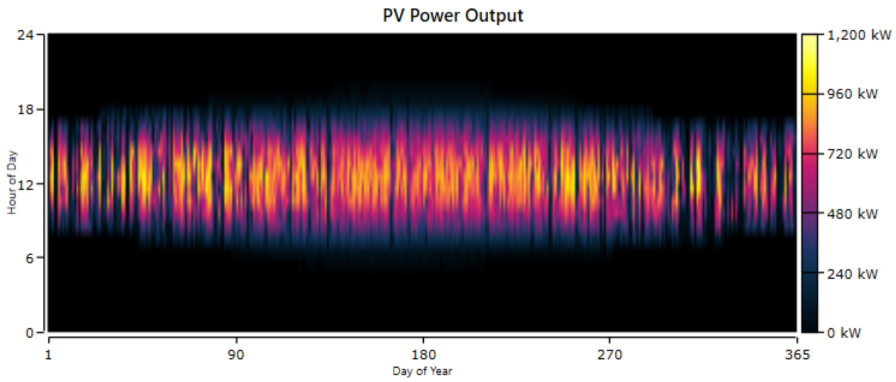

Figure B.2: Performance of PV Modules

B.3. Wind Turbine Power Production - Renewable Energy Communities

Quantity	Value	Units
Total Rated Capacity	900	kW
Mean Output	195	kW
Capacity Factor	21.7	%
Total Production	1,710,012	kWh/yr

Quantity	Value	Units
Minimum Output	0	kW
Maximum Output	910	kW
Wind Penetration	78.1	%
Hours of Operation	7,485	hrs/yr
Levelized Cost	0.0987	€/kWh

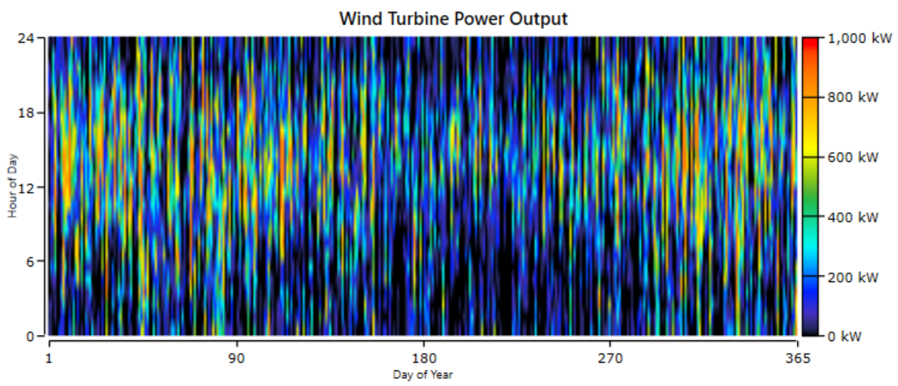

Figure B.3: Performance of wind turbines

Notes: the wind turbine's capacity factor given by Homer Pro is incorrect. Indeed, it considers the device as having a nominal capacity of 900 kW. This follows the absence of a DW61-1 MW in the available database. Consequently, a DW61-900 kW has been selected, to later modify its power curve and align it to the correct one. The production profile thus reflects the realistic one; at the contrary, the nominal capacity is still memorised as being 900 kW.

B.4. Exchange with the Grid - Renewable Energy Communities

Month	Energy Purchased (kWh)	Energy Sold (kWh)	Net Energy Purchased (kWh)	Peak Load (kW)	Energy Charge €	Demand Charge €
April	58,187	213,072	-154,886	278	-€11,524.1	€0
May	61,858	184,376	-122,518	284	-€9,969.93	€0
June	61,391	173,747	-112,356	279	-€9,394.63	€0
July	67,475	175,635	-108,159	274	-€9,551.21	€0
August	75,482	160,233	-84,751	287	-€8,690.60	€0
September	71,172	155,255	-84,083	278	-€8,412.03	€0
October	66,695	156,021	-89,326	280	-€8,451.93	€0
November	63,809	160,706	-96,897	290	-€8,625.03	€0
December	59,834	160,393	-100,560	288	-€8,569.89	€0
Annual	765,452	2,089,250	-1,323,798	291	-€112,894.	€0

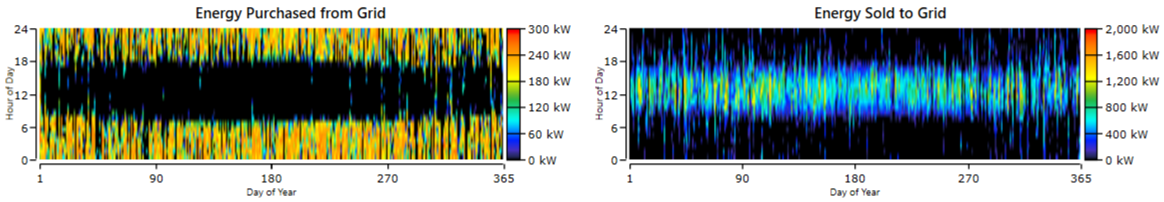

Figure B.4: Exchange with the grid

B.5. Costs Summary - Renewable Energy Communities

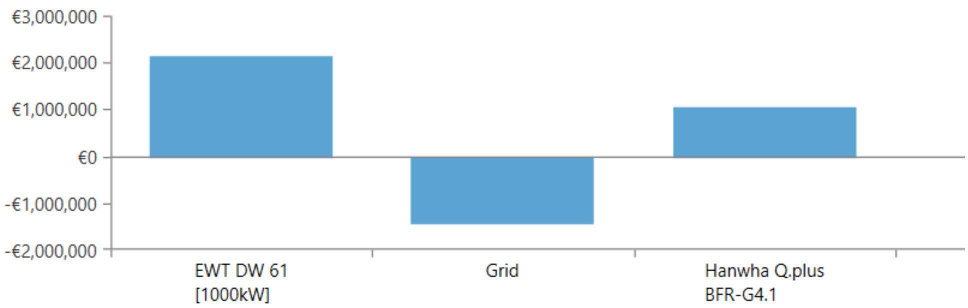

Component	Capital (€)	Replacement (€)	O&M (€)	Fuel (€)	Salvage (€)	Total (€)
EWT DW 61 [1000kW]	€1,454,719.00	€0.00	€727,224.52	€0.00	€0.00	€2,181,943.52
Grid	€0.00	€0.00	-€1,459,451.69	€0.00	€0.00	-€1,459,451.69
Hanwha Q.plus BFR-G4.1	€947,000.00	€0.00	€114,667.07	€0.00	€0.00	€1,061,667.07
System Converter	€1.10	€0.00	€0.00	€0.00	€0.00	€1.10
System	€2,401,720.10	€0.00	-€617,560.11	€0.00	€0.00	€1,784,160.00

Figure B.5: Actualised costs summary

Note: the cost of the converter is shown to be 1.10 €, seen the impossibility of setting it null. In the made optimisation framework, the cost of the converter is indeed heeded in that of the batteries and PV panels.

B.6. Electrical Load - Autonomous Systems

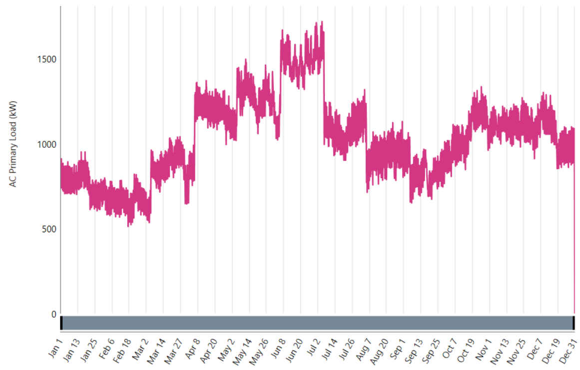

Figure B.6: Electrical load yearly pattern

B.7. PV Modules Power Production - Autonomous Systems

Quantity	Value	Units
Rated Capacity	587	kW
Mean Output	107	kW
Mean Output	2,575	kWh/d
Capacity Factor	18.3	%
Total Production	939,925	kWh/yr

Quantity	Value	Units
Minimum Output	0	kW
Maximum Output	751	kW
PV Penetration	10.5	%
Hours of Operation	4,384	hrs/yr
Levelized Cost	0.115	€/kWh

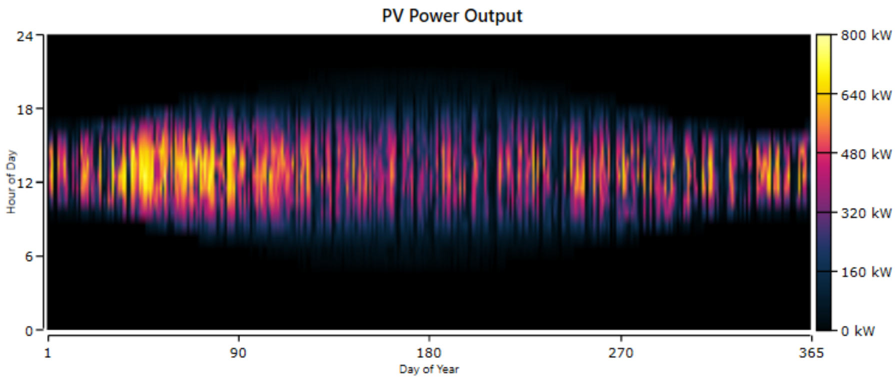

Figure B.7: Performance of PV Modules

B.8. Wind Turbine Power Production - Autonomous Systems

Quantity	Value	Units
Total Rated Capacity	900	kW
Mean Output	243	kW
Capacity Factor	27.0	%
Total Production	2,131,602	kWh/yr

Quantity	Value	Units
Minimum Output	0	kW
Maximum Output	974	kW
Wind Penetration	23.7	%
Hours of Operation	6,992	hrs/yr
Levelized Cost	0.151	€/kWh

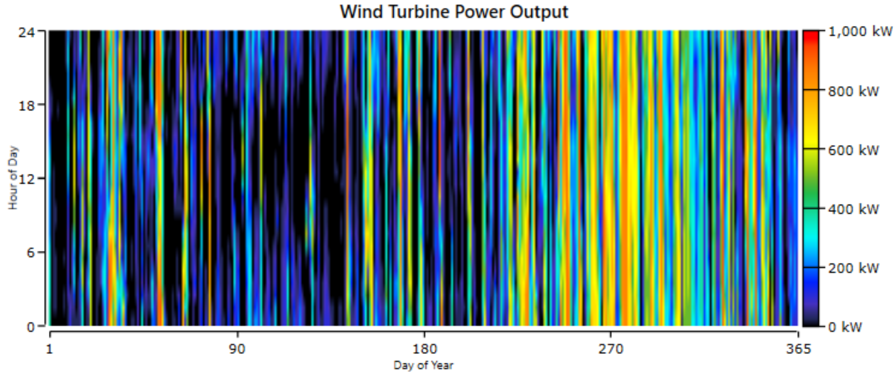

Figure B.8: Performance of wind turbines

Notes: the wind turbine's capacity factor given by Homer Pro is incorrect. Indeed, it considers the device as having a nominal capacity of 900 kW. This follows the absence of a DW61-1 MW in the available database. Consequently, a DW61-900 kW has been selected, to later modify its power curve and align it to the correct one. The production profile thus reflects the realistic one; at the contrary, the nominal capacity is still memorised as being 900 kW.